

# A QUANTILE REGRESSION APPROACH TO DEFINE OPTIMAL ECOLOGICAL NICHE (HABITAT SUITABILITY) OF COCKLE POPULATIONS (*CERASTODERMA EDULE*)

Amélie Lehuen<sup>a\*</sup>, Chloé Dancie<sup>b</sup>, Florent Grasso<sup>c</sup>, Francis Orvain<sup>a</sup>

<sup>a</sup> Biologie des Organismes et Ecosystèmes Aquatiques (BOREA) Université de Caen Normandie UNICAEN, Sorbonne Université, MNHN, UPMC Univ Paris 06, UA, CNRS 8067, IRD, Esplanade de la paix, F-14032 Caen, France

<sup>b</sup> CSLN, Cellule de Suivi du Littoral Normand (CSLN), 53 rue de Prony, 76600 Le Havre, France

<sup>c</sup> Ifremer, DYNECO/DHYSED, F-29280 Plouzané, France.

\* Corresponding author: [amelie.lehuen@gmail.com](mailto:amelie.lehuen@gmail.com)

## Abstract

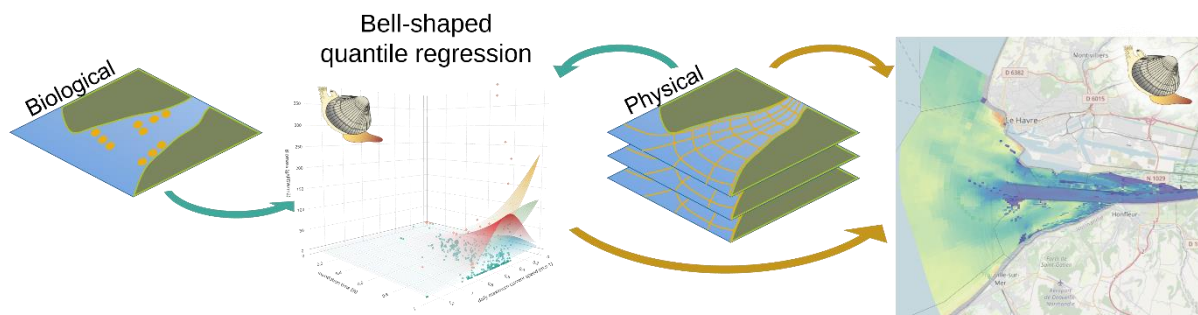
For several decades now, species distribution models (SDMs) have been a promising area of ecological research. The aim of the present study is to define optimal ecological niches and habitat suitability for the population of the bivalve *Cerastoderma edule* in the Seine estuary. The method involved applying quantile regression to a 20-year biological dataset at the scale of the estuary, coupled with a hydro-morpho-sedimentary model data set validated over a longer period (25 years) also at the scale of the estuary, using 100-m mesh cells. This study was carried out to describe biological responses to environmental factors involved in defining an optimal ecological niche, using the bifactorial Gaussian equation using physical forcings (tidal currents, bed shear stress, etc.) as explanatory factors. On the basis of a preliminary multivariate analysis of the physical descriptors, a comparison was made between three different types of equation (linear, B-spline and Gaussian) in four sets of paired environmental factors: daily maximum current speed & inundation time, daily salinity range & temperature, daily salinity range & bathymetry, daily maximum bed shear stress & mud content. The non-linear quantile regression with a bifactorial Gaussian equation produced the best description of habitat suitability and optimal niches, at the 95<sup>th</sup> centile and using the biomass (gAFDW/m<sup>2</sup> - Ash Free Dry weight). Daily maximum current speed & inundation time and daily salinity range & temperature were the most pertinent SDMs. The optimal ecological niche for *C. edule* appeared to be lower intertidal marine areas, with temperate and low dynamic waters, settled in muddy sand sediment of the tidal flats of Seine estuary. Using this technique, the calculation of optimal niches in this ecosystem was explored over a period of 25 years and analysed in isolated sectors and can now be applied in different scenarios related to the global

32 warming. We propose several reliable models, so that different kinds of prediction can now be applied  
33 according to the context of future scenarios.

## 34 Highlights

- 35 • Bifactorial gaussian quantile regression, with a high quantile, e.g. the 95<sup>th</sup> centile, is performant  
36 to express the optimal ecological niche of *C. edule* at the scale of the estuary.
- 37 • Daily maximum current speed and inundation time are the most adequate factors to describe  
38 the estuary, thus to build an SDM.
- 39 • Suitability index was built based on optimal ecological niches to assess habitability of areas in  
40 the Seine estuary.
- 41 • Optimal *Cerastoderma edule* conditions correspond to low intertidal marine shores, temperate  
42 and moderate currents in muddy sand sediment.

## 43 Graphical abstract



44

## 45 Keywords

46 *Cerastoderma edule*, quantile regression, species distribution model, optimum ecological niches,  
47 habitat suitability

## 48 Manuscript

### 49 1 Introduction

50 Understanding the links and interactions between abiotic and biotic components is necessary to  
51 preserve and restore areas affected by environmental fluctuations caused by human activity, and to

52 conserve the benefits of their ecosystem services (Richards and Lavorel, 2023). The concept of  
53 ecological niches was defined to better understand and predict the population dynamics (Hutchinson,  
54 1957). Hutchinson conceptualised an ecological niche as "the n-dimensional set of environmental  
55 conditions that allow a species to live and reproduce".

56 A species distribution model (SDM) is an approach providing practical information on the spatial  
57 distribution of species based on ecological niche modelling. The construction of an SDM requires the  
58 definition and selection of three main components: 1) an ecological model that brings context to the way  
59 the SDM will be produced and analysed; 2) a data model defining how the data are collected and  
60 prepared; 3) a statistical model involving the choice of statistical method, error function and significance  
61 tests (Austin, 2007, 2002).

62 A wide choice of statistical models for constructing SDM is available, with two main categories: the  
63 correlative ones (Austin, 2002; Guisan and Zimmermann, 2000) and the mechanistic ones (Kearney  
64 and Porter, 2009). Each approach has advantages and disadvantages (Kearney and Porter, 2009; Melo-  
65 Merino et al., 2020), but the vast majority of studies carried out to date are correlative (Robinson et al.,  
66 2011). Correlative SDMs link the presence or abundance of a species with spatial habitat data, thereby  
67 quantifying the relation between environmental factors and species distributions. The model define an  
68 environmental profile on an empirical basis, making it possible to define the abiotic factors determining  
69 the maintenance of a species and to infer its presence or absence in areas where no biological data are  
70 available, or the impact of changing abiotic conditions (Elith and Leathwick, 2009; Franklin, 2010; Guisan  
71 and Thuiller, 2005). These methods generally use geolocalised biological data of a species and abiotic  
72 parameters measured by techniques such as field or remote measurements or modelling (Brown et al.,  
73 1996; Guisan and Zimmermann, 2000; Melo-Merino et al., 2020; Van Der Wal et al., 2008).

74 Various and increasing statistical tools can be used with correlative SDMs, among them the  
75 regressions are often based on either Ordinary Least Square (OLS) or Generalized Linear Models  
76 (GLMs, fitted by Maximum Likelihood Estimation), which describe the distribution of biological response  
77 with the chosen abiotic predictors (Bolker et al., 2009; Robinson et al., 2017). These approaches provide  
78 access to a level of information that is rather complex to interpret, given the patchy spatial distribution  
79 of many species, variations in recruitment from one year to the next, and the complex life cycles of some  
80 species (Ysebaert and Herman, 2002). In particular, the construction of a SDM based on several abiotic  
81 measurements cannot account for other factors, either because they are not available or are not known.  
82 Those factors may have a limiting effect on the biological response which will then reflect the response  
83 to these unknown limiting factors. This is the statement of Liebig's law of minima: if other resources are  
84 not optimal for certain observations, the measured response of the species will be less than the  
85 maximum possible response to the observed resource. As a result, OLS or GLM models incorporate the  
86 effects of unmeasured limiting factors on the SDM (Austin, 2007; Cade et al., 1999).

87 Quantile regression (QR) is defined as a sequence of ascending envelopes that cover an increasing  
88 proportion of occurrence according to quantiles (Koenker and Hallock, 2000; Koenker and Machado,  
89 1999). Studies have been conducted for more than 40 years to carry out QR, and recent advances in  
90 computer tools have improved its use, refined the performance indicators, and facilitated its

91 interpretation especially for ecological applications, such as SDM (Austin, 2007; Cade et al., 2005, 1999;  
92 Cade and Noon, 2003). When the time scale is long, we can admit that there is one real probability that  
93 the population express its maximum response at a moment (“when all planets are aligned”). By targeting  
94 the upper quantiles of the distribution in long-term surveys, it is possible to define the best maximum  
95 biological response to abiotic predictors, with any other factors, whether biological, environmental or  
96 mobility, that are not accounted for, being considered as non-limiting (Schröder et al., 2005). The use  
97 of QR in a correlative SDM with a sufficiently rich database and over a sufficiently long period of time,  
98 makes it possible to define the optimal conditions for a species with respect to selected abiotic factors,  
99 freeing it from particular recorded conditions (meteorological conditions, sanitary events, lifespans). In  
100 addition, the effects of interaction between species, with their environment and the biogeochemical  
101 processes they generate can make environments more dynamic and welcoming on a very local scale,  
102 through a system of self-organisation. This can lead to very high densities of a species in a local 'patch',  
103 a phenomenon often observed in estuarine environments. Thrush modelled species distributions based  
104 on the maximum density of intertidal species (Thrush et al., 2003). Quantile regression follows the same  
105 principle, but is less 'optimistic', because it is unlikely that the extreme densities measured at a very  
106 local level can be extended to larger scales with the same amplitude. In other words, the variability  
107 observed below the upper quantiles is related to factors that are not observed and above the upper  
108 quantiles reflects the auto-organisation processes of biological populations (Weerman et al., 2011,  
109 2010). In this way, a correlative SDM with QR get close to the main impacts of abiotic factors on the  
110 biological response, thus defining the optimal ecological niche. What is more, using abundance or  
111 biomass as the biological response, one obtains more than a specific geographical range based on  
112 presence/absence. Biomass is rather related to the growth and aging ability of individuals, whereas  
113 density rather indicates the patchiness of distribution and the effect of recruitment. Both are  
114 consequently meaningful to study how long a population live.

115 Considerable work has been invested in SDM for many years, but only recently included marine  
116 environments, and the focus was more on pelagic areas (Melo-Merino et al., 2020; Robinson et al.,  
117 2011, 2017), whereas intertidal and estuarine areas were less studied. Brown et al. mentioned the  
118 importance of ecological gradients (Brown et al., 1996), estuarine and intertidal environments are  
119 undeniably subject to massive, repeated and frequent gradients, due to the action of the tide and the  
120 influence of the river, both of which have major impacts on abiotic factors. However, the challenges of  
121 managing estuaries and coasts in the context of climate change and anthropogenic pressure are key  
122 issues (Crossland et al., 2005; Grassle, 2013). With respect to ecosystem services, among other things,  
123 an estuary is a shipping lane, a fishing ground and an area comprising diverse natural habitats. All these  
124 activities compete for space and have different needs and yet are linked to each other, so there is a  
125 need for decision support tools that improve their management and foresee their future development  
126 (Degraer et al., 2008; He et al., 2015; Schickele et al., 2020). The vulnerability of estuarine sediments  
127 to the sea level increase is studied for a long time (Healy et al., 2002) and it is very relevant to focus on  
128 the response of the benthic macrozoobenthos not only to temperature or salinity changes, but also to  
129 physical dynamics (current velocity, bed shear stress, sediment composition).

130 In estuarine ecosystems, benthic macrofauna (or macrozoobenthos) is found at different levels  
131 depending on the trophic guild to which it belongs (Dubois et al., 2007; Saint-Béat et al., 2013). The  
132 capacity of benthic macrofauna to resist external stressors is yet not fully understood, but abiotic factors  
133 are habitat-defining parameters on which a cohort of species depends (Ysebaert and Herman, 2002).  
134 In particular, sediment and hydrological parameters have a direct impact on the activity and spatial  
135 distribution of macrozoobenthos, with sediment acting as a food source, habitat, shelter and breeding  
136 ground but which can also cause discomfort. Sediment indicators, including grain size median and fine  
137 silt content, have been shown to strongly contribute to explaining variations in macrozoobenthic  
138 communities (Anderson, 2008; Thrush et al., 2005, 2003). The benthic macrofauna of the Seine Bay  
139 (Normandy, France) has been extensively studied in recent decades (Bacouillard et al., 2020; Baffreau  
140 et al., 2017; Dauvin, 2015; Le Guen et al., 2019) and estuarine management included in subsequent  
141 regional program frameworks (<https://www.seine-aval.fr/>). Accessing abiotic factors, and especially  
142 physical forcings, in an estuary is a challenge that can be solved by developing hydro-morpho-  
143 sedimentary (HMS) models, which use principles of fluid and particle physics to define the parameters  
144 of interest in the estuary at an intermediate scale. The Seine estuary (Normandy, France) was the  
145 subject of the Mars3D model adjustment, which describes the dynamics of the physical parameters in  
146 an estuary, such as bottom elevation, salinity, temperature, current velocity, water surface elevation,  
147 with a particular effort invested in describing the erosion, deposition and consolidation properties of  
148 sand-mud mixtures (Grasso et al., 2021, 2018; Grasso and Le Hir, 2019; Mengual et al., 2020; Schulz  
149 et al., 2018). Such tools allow a temporal projection at a regional spatial scale and hence to make  
150 projections based on different sets.

151 In a similar intertidal environment, examples of correlative SDMs using QR were developed by  
152 (Cozzoli et al., 2017, 2014, 2013). Indeed, using a long series of benthic macrofauna sampling  
153 campaigns in the Oosterschelde estuary (The Netherlands), and an HMS model in the same area, the  
154 SDM with QR above the 90<sup>th</sup> percentile enabled identification of the optimal conditions for biological  
155 response, in this case biomass, according to annual averages of the chosen factors. The authors  
156 characterize this model as habitat suitability or potential niche. By modelling a type of habitat rather than  
157 a biological response, this type of model reduces inter-annual variations caused by many unmeasured  
158 factors, is more informative about the environment under study, and provides a more functional  
159 management guide. Habitat suitability, i.e., relationships that describe physical-biological coupling, can  
160 then be used to understand the long-term and large-scale evolution of benthic species in response to  
161 changes in abiotic conditions, whether natural, anthropogenic, or due to climate change.

162 In practice, correlative SDM with QR does not presuppose the type of equation that links abiotic  
163 factors to a biological response, or even the number of predictors to be used. This method can be used  
164 together with an expected response curve for each factor. It was observed that the biological response  
165 to physical factor is often non-linear, and can be modelled by a Gaussian distribution (Huisman et al.,  
166 1993; Van Der Wal et al., 2008). In the present study, we built a SDM for an optimal ecological niche,  
167 to analyse the links between the spatial distribution of species and the physical characteristics of their  
168 habitat. The model consists in a correlative SDM based on QR (the statistical model) that provides a  
169 spatial description of the gradient of the best biological response (maximal occurrence) in regard of

170 selected abiotic factors generated by a hydro-morpho-sedimentary model. Using the *Cerastoderma*  
171 *edule*, the common cockle, as an example, the study compares the performances and results of linear,  
172 Gaussian and B-spline QR models as ecological models. Several combinations of abiotic factors were  
173 chosen because as mentioned in (Guisan and Zimmermann, 2000) "Nature is too complex and  
174 heterogeneous to be predicted accurately in every aspect of time and space from a single, although  
175 complex, model". After applying a multivariate analysis (PCA) on physical descriptors, four sets based  
176 on combinations of two abiotic factors were processed because they can answer different ecological  
177 questions: daily maximum current speed & inundation time, daily salinity range & water temperature,  
178 daily salinity range & bathymetry, daily maximum bed shear stress & mud content. These models were  
179 geographically applied and analysed. A suitability index is also proposed as a tool for the management  
180 of estuarine ecological areas.

181

## 182 2 Materials and Methods

183 All data processing was conducted in R version 4.2.2 (2022-10-31 ucrt) except for Mars3D pre-  
184 treatment in Matlab 2019a. Significance levels are  $p < .0001$  with "\*\*\*\*",  $p < .001$  with "\*\*\*",  $p < .01$  with  
185 "\*\*",  $p < .05$  with "\*".

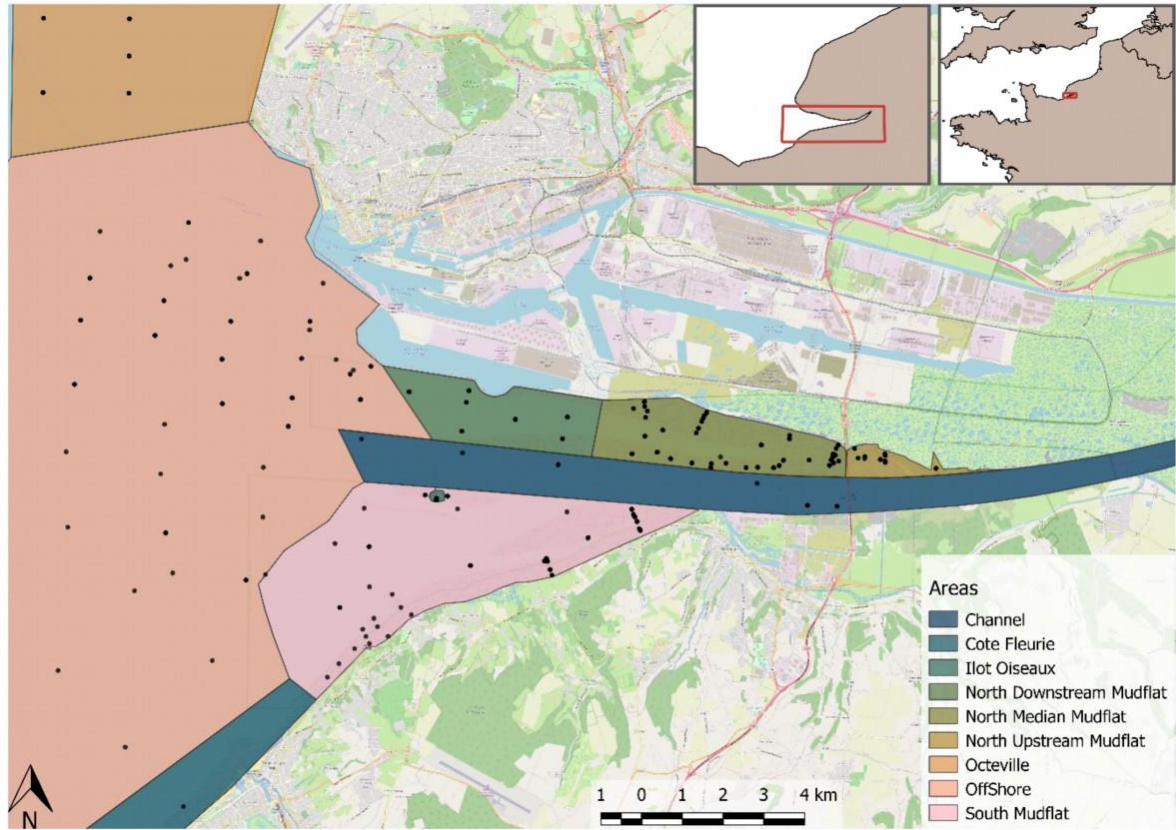
### 186 2.1 Study area

187 The Seine estuary in Normandy, north-western France, is defined as the last 170 km of the river  
188 leading to the marine ecosystem close to Le Havre, it starts at Poses weir upstream and ends in the  
189 Seine Bay downstream. The Seine estuary is macrotidal (tidal range up to 8 m), and is subject to fresh  
190 water inflows ranging from 100 to more than 1000  $\text{m}^3 \cdot \text{s}^{-1}$ , with a mean of 450  $\text{m}^3 \cdot \text{s}^{-1}$  in the two last  
191 decades. Tidal dynamics and the wave regime have a significant impact on the hydro-sedimentary  
192 dynamics of the mouth of the estuary (Grasso et al., 2021; Schulz et al., 2018).

193 The mouth of the estuary hosts a variety of habitats that provide many ecosystem services (Beck et  
194 al., 2001; Boesch and Turner, 1984). In particular, intertidal mudflats play a crucial role in the Seine  
195 estuary and are areas of major interest including for nutrient recycling, coastline protection and as  
196 feeding / nesting sites for migratory birds. The Seine estuary is marked by structures that have  
197 profoundly modified this ecosystem, which is still undergoing changes that began at the beginning of  
198 the 20<sup>th</sup> century (Lesourd et al., 2016). Numerous dykes have been built and dredging has been carried  
199 out to increase the capacity of the navigation channel, which contributed to the disconnection of the two  
200 banks of the estuary and reduced the extent of wetlands. Among these works, some were huge projects  
201 construction of Normandy Bridge (1989-1995), which crosses the Seine estuary and the "Port 2000"  
202 project (2000-2005) to enlarge the port of Le Havre, mainly to allow large container ships to access new  
203 all-day loading platforms.

204 The Port 2000 project involved ecological compensation in the form of the creation of a nature  
205 reserve in 1997, as well as the digging and dredging of an artificial channel in the north upstream mudflat

206 and the creation of a small island (Ilot Oiseaux) for migratory birds in the southern mudflat (Aulert et al.,  
207 2009). Several historically known areas in the Seine estuary that differ in either their habitat or  
208 community have been studied, mainly mudflats and subtidal areas (Morelle et al., 2020; Tecchio et al.,  
209 2016) (Figure 1).



210

211 *Figure 1 Maps showing the habitats defined in the dataset of the study area. Dots represent the*  
212 *location of the biological samples.*

## 213 2.2 Biological model

214 The cockle *Cerastoderma edule* (Linnaeus, 1758) is a bivalve belonging to the family of Cardiidae  
215 which is widely distributed and exploited in waters off northern Europe up to north Iceland and off the  
216 coast of West Africa down to southern Senegal (Hayward and Ryland, 1995). The oval ribbed shells of  
217 the cockle can reach 6 cm in diameter and are white, yellowish or brown in colour, and its lifespan is 2-  
218 3 years (Malham et al., 2012). Cockles are suspension-feeders, inhabiting the few uppermost  
219 centimetres of the sediment with its two siphons emerging from the surface. Its growth depends mainly  
220 on microphytobenthos in the juvenile stage and on trophic phytoplankton in the adult stage (Sauriau and  
221 Kang, 2000).

222 Cockle habitats are located in the central areas of the foreshore subject to medium currents (between  
223 0.3 and 0.7 m.s<sup>-1</sup> of maximum tidal current speed) (Herman et al., 1999; Ysebaert et al., 2002), typical  
224 marine salinity (> 30) and they prefer fine sands (slightly silty, grain size between 100 and 200 μm)  
225 (Cozzoli et al., 2014; Ubertini et al., 2012). This species can be found at particularly high densities in the  
226 English Channel, the most densely inhabited area being the Bay of Veys, (density in the order of 200 to



227 500 ind.m<sup>-2</sup>), and may exceptionally exceed 5000 ind.m<sup>-2</sup> (Gosling, 2003; Mahony et al., 2022). Winter  
228 conditions, current intensity and stress (erosion) appear to explain the high mortality rates observed in  
229 some years (Herman et al., 1999; Van Colen et al., 2010).

## 230 2.3 Datasets

### 231 2.3.1 Biological data

232 Data concerning the benthic macrofauna of the Seine Bay are grouped in a database named  
233 *MAcrobenthos Baie et Estuaire de Seine* (MABES) (Dauvin et al., 2006; L'Ebrelec et al., 2019). This  
234 dataset provides information on sampling (geolocation, sampling method) and fauna (density [ind.m<sup>-2</sup>],  
235 biomass [gAFDW.m<sup>-2</sup>] – Ash Free Dry Weight) collected in several projects for the past 40 years. This  
236 database was completed with data from the *Cellule de Suivi du Littoral Normand* (CSLN) surveys  
237 conducted for the *Maison de l'Estuaire*.

238 The raw data (n = 50,948) were harmonised and grouped in a single database which contain a total  
239 of 31,079 observations, and 187 sampling stations (with some variation in coordinates from year to  
240 year), with an average of 87 stations sampled in each campaign (depending of the project), mainly in  
241 September, October, and November. A series of 5-year periods was chosen among the periods covered  
242 by the dataset, from 2000 to 2019 (the years before 2000 were discarded as they contained too few  
243 observations, n = 216), with only one or two sampling campaigns per year: 2000-2005, including the  
244 construction of 'Port 2000' which caused major disruptions in the estuary; 2006-2010; 2011-2015; 2016-  
245 2019. A total of 627 different species are contained in the records.

### 246 2.3.2 Hydro-Morpho-Sedimentary data

247 The HMS dataset was generated during the ARES project using the Mars3D model (Grasso et al.,  
248 2021, 2019). Mars3D can be used in the context of estuarine hydrodynamics and application to fine  
249 sediment and sand transport. This three-dimensional (3D) process-based model was set up and run  
250 under realistic forcings (including tide, waves, wind, and river discharge). The Mars3D model is  
251 composed of the hydrodynamic core forced by the WAVEWATCHIII® wave model (Roland and Arduin,  
252 2014) coupled with the MUSTANG sediment module (erosion, deposition, consolidation...). MUSTANG  
253 accounts for spatial and temporal variations in sand and mud content in the multi-layer sediment bed,  
254 as well as for consolidation processes, and also resolves advection/diffusion equations for different  
255 classes of particles in the water column (Grasso et al., 2018; Le Hir et al., 2011; Mengual et al., 2020).

256 The ARES dataset covers the simulation periods 1990-2000 and 2005-2018. The period 2001-2004  
257 was not modelled because it corresponds to the period of construction of the Port 2000 project. The  
258 dataset outputs are available at intervals of 30 minutes for the entire Seine Bay area each hydrological  
259 year, starting on October 1<sup>st</sup> and finishing on September 30<sup>th</sup>. The hydrological sub-data contain 58  
260 variables, some of which depend on water depth, with 10 levels in the water column, of which only the  
261 median of the 3 lower layers were retained to reflect benthic conditions: current speed, temperature,  
262 salinity and SPM for 5 particles sizes. The other variables retained are bathymetry and the inundation



263 rate calculated from bathymetry and water height. The sedimentary sub-data contain 19 variables, some  
264 of which depend on the depth in the sediment, with 6 levels corresponding to 1 m, of which only the  
265 median of the 4 upper layers is retained, i.e. 10 cm to reflect benthic conditions: temperature, salinity  
266 and sediment concentration for 5 particles sizes. The other variables retained are the total thickness of  
267 the sediment and the bed shear stress.

268 In addition to these variables, processing was carried out to extract other information. The daily  
269 maximum was calculated for current speed and bed shear stress, the daily range was calculated for  
270 salinity and temperature, and the yearly sediment budget was calculated from the variation in sediment  
271 thickness at the beginning and end of the year. The sediment total concentration is the sum of all  
272 sediment concentrations, and the mud content was deduced from the different particle size  
273 concentrations. All the variables selected and created, 14 in all, were brought down to a median  
274 calculated over the hydrological year.

275 The 14 abiotic factors were studied to select the most relevant factors and limit their number to avoid  
276 autocorrelations. A PCA (`FactoMineR::PCA` and `factoextra` package for visualisation) based on a  
277 correlation matrix was carried out on all the factors, allowing complementary parameters to be identified  
278 on the two main axes. In addition, a correlation matrix provides a complementary view of the dataset,  
279 including the biomass and density of *C. edule* to ensure that there is no direct correlation between abiotic  
280 and biotic factors. Based on those analyses, 4 couples of abiotic factors were chosen.

## 281 2.4 Model adjustments

### 282 2.4.1 Quantile regression

283 The quantile regression (QR) mathematical theory has been extensively expanded and described by  
284 Koenker in recent decades (Koenker, 2019; Koenker et al., 2019; Koenker and Bassett, 1978; Koenker  
285 and Hallock, 2000, 2001; Koenker and Machado, 1999). Its use in ecological studies has increased  
286 significantly since the work of Cade and Noon (Cade et al., 2005, 1999; Cade and Noon, 2003).

287 Three different types of models were defined in this study (Table 1), all using two abiotic factors, but  
288 with different functions to link them to the biological response. Mathematical notation is based on (1) the  
289  $\tau$  subscript for variables that are quantile-dependent, (2)  $\beta$  for model coefficients, that are vectors of  
290 length  $\tau$ , (3)  $\mu$  and  $\sigma$  for mean and standard deviation. QR were performed with the *quantreg* package in  
291 R developed by Koenker. The three model types were computed with different quantiles  $\tau = [0.5, 0.9,$   
292  $0.95, 0.975]$ , 0.5 being the equivalent of an OLS regression, and kept as a reference, the other values  
293 higher than 0.9 to seek for the optimum response.

294 The model was adjusted on the biological data with an associated HMS cell to create SDMs, which  
295 were then applied to the HMS data set, focused on the estuary. The maximum of the SDM niche  
296 response was used to normalize the model response, to create a suitability index, ranging from 0 to 1.

297 *Table 1 List of types of models tested*

Name	Type	Equation	Rationale
RQ2int	RQ linear with interaction	$y_{\tau} = \beta_{0\tau} + \beta_{1\tau} \cdot x_1 + \beta_{2\tau} \cdot x_2 + \beta_{3\tau} \cdot x_1 \cdot x_2$ <code>quantreg::rq(x1*x2)</code>	Comparison with the results in (Cozzoli et al., 2014)
RQ2nli	RQ bifactorial gaussian (non-linear)	$y_{\tau} = A \cdot e^{-\left[ \frac{(x_1 - \mu_{1\tau})^2}{2 \cdot \sigma_{1\tau}^2} + \frac{(x_2 - \mu_{2\tau})^2}{2 \cdot \sigma_{2\tau}^2} \right]}$ <code>quantreg::nlrq(f(x1, x2, initial.conditions))</code>	With $\mu$ and $\sigma$ initiated by the mean and the standard deviation for each predictor (Huisman et al., 1993; Schröder et al., 2005).
RQ2bsp	RQ linear with B-Spline	<code>quantreg::rq(splines::bs(x1, degree=3, knots=median(x1)) * bs(x2, degree=3, knots=median(x2)))</code>	Avoid pre-determined shape of the equation and the use of a non-linear function (Cozzoli et al., 2013)

## 298 2.4.2 Model selection

299 QR model validation was based on the Akaike Information Criterion (AIC). This index evaluates the  
300 performance of the model using the fewest possible predictors (Akaike, 1974), and was adapted to the  
301 QR (Cade et al., 2005), named AICc, and the delta with the minimum of the model series was processed  
302 ( $\Delta AICc$ ). Following Koenker's recommendation, the  $R^1$ , equivalent to OLS  $R^2$  developed by Koenker and  
303 Machado (Koenker and Machado, 1999), was not used (Koenker, 2006).

304 In addition to AICc, the relationship between predicted and observed values was plotted. The  
305 predicted (model output) data were discretized in 10 homogeneous classes and for each class, the  
306 corresponding sample quantile of the observed data was calculated, with a bootstrap (R=1000) to cope  
307 with the limited number of records. To assess the validity of the model, a linear correlation was drawn  
308 for each quantile.

## 309 3 Results

310 High resolution and interactive figures are in the supplementary data in [https://am-](https://am-lh.github.io/Melting_pot/SDM/SDM_Suppl_Data.html)  
311 [lh.github.io/Melting\\_pot/SDM/SDM\\_Suppl\\_Data.html](https://am-lh.github.io/Melting_pot/SDM/SDM_Suppl_Data.html).

### 312 3.1 Description of the biological data set

313 Biological data for *C. edule* comprised a total of  $n = 543$  observations. The observations were split  
314 into periods: 2000-2005 ( $n = 108$ ), 2006-2010 ( $n = 155$ ), 2011-2015 ( $n = 174$ ), 2015-2019 ( $n = 106$ ). The  
315 following treatment focussed on the mudflats used by *C. edule* (south mudflat ( $n = 218$ ), north median  
316 mudflat ( $n = 198$ ), north downstream mudflat ( $n = 82$ ), north upstream mudflat ( $n = 2$ )). Differences in  
317 biomass and density are detailed as a function of the period and the different areas concerned (Supp.  
318 Data 3.1). The only noticeable spatial and temporal differences concerned biomass in the south mudflat  
319 and the north (median and downstream) mudflats in the period 2000-2005.

## 320 3.2 Selection of the Hydro-Morpho-Sedimentary factors and their association

321 The PCA analysis on physical descriptors (Figure 2, Supp Data 3.2, detailed scores Table 2) gives  
322 3 main dimensions for a total variance of 65.4 % (PC1 = 28.8 %, PC2 = 20.7 %, PC3 = 15.9 %):

- 323 • PC1 corresponds to the hydrodynamics of the area with the contributions of: daily maximum  
324 current speed (19.6 %), current speed (17.8 %), daily salinity range (17.8 %), daily maximum  
325 bed shear stress (10.9 %), MES mud (9.2 %), bed shear stress (8.7 %).
- 326 • PC2 is related to the morphology of the estuary: inundation time (23.1 %), daily temperature  
327 range (20.4 %), bathymetry (19.9 %), salinity (14 %), temperature (8.3 %).
- 328 • PC3 describes the sediments characteristics of the bed: sediment total concentration (30.2  
329 %), mud content (29 %), bed shear stress (18 %), daily maximum bed shear stress (7.2 %).

330 Considering those axes, sets were built with two abiotic factors from different axis to more accurately  
331 describe the environment. The sets tested were:

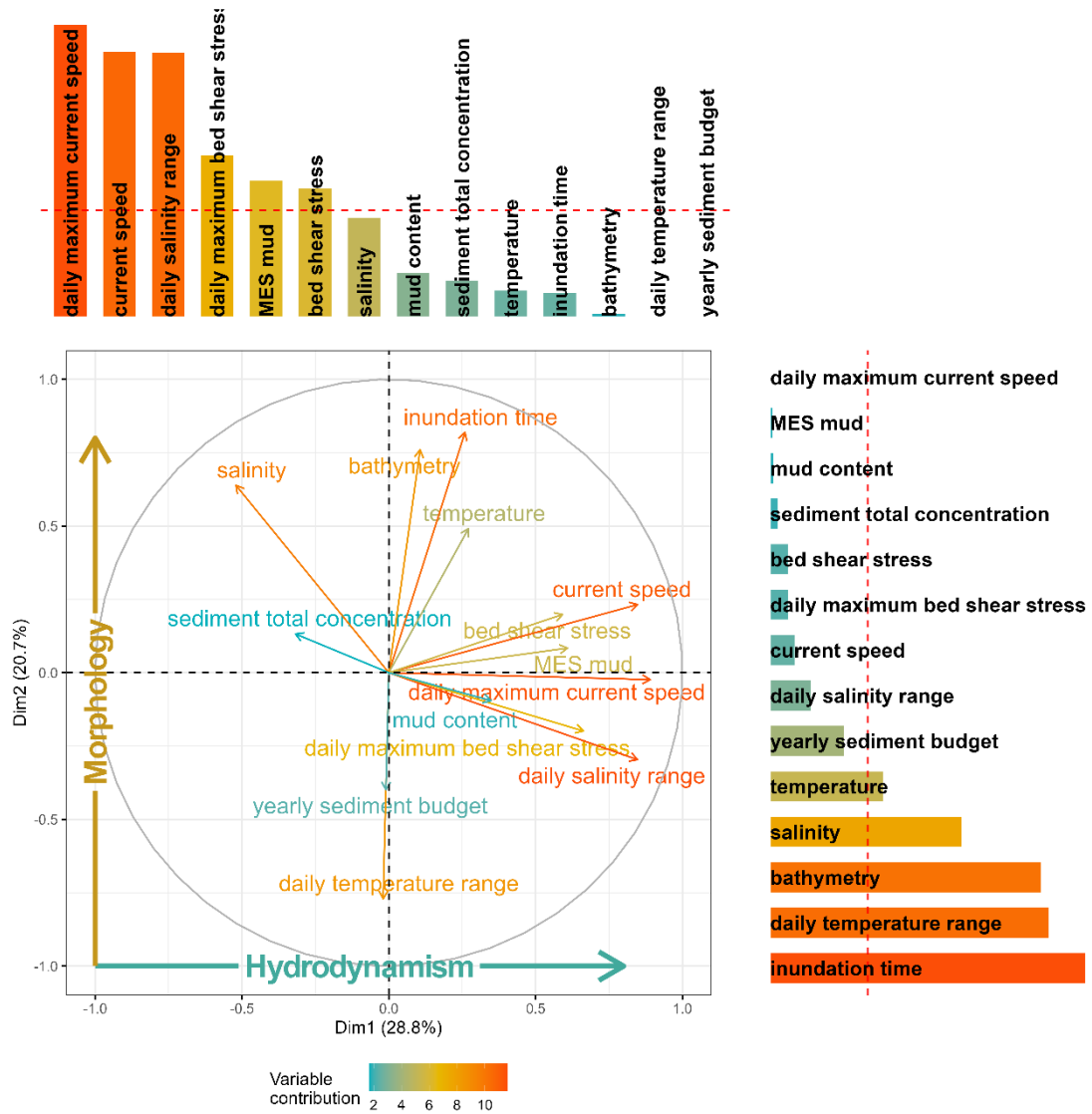
332 A. Daily maximum current speed [ $\text{m}\cdot\text{s}^{-1}$ ] & inundation time [%] – PC1-PC2: These variables are  
333 the main contributors of the two firsts axes, are easily retrieved at high frequency and enable  
334 comparison with the study by Cozzoli et al. (Cozzoli et al., 2014). They are also interesting  
335 because they contain information on the localisation of the tidal area that could evolve with  
336 sea level rise and information on the hydrological conditions including fluctuations in the flow  
337 rate of the river linked to climate change. A significant correlation was observed between  
338 these two variables in the HMS dataset ( $R^2 = 0.56^{****}$ ).

339 B. Daily salinity range & temperature [ $^{\circ}\text{C}$ ] – PC1-PC2: These factors are easily measurable at  
340 high frequency (Goberville et al., 2010) and are not correlated ( $R^2 = 0.02$  ns). They illustrate  
341 two aspects of climate change: changes in the river regime which have an impact on the  
342 salinity profile of the estuary (Lheureux et al., 2022), and variations in water temperature  
343 (globally increase), to which species must gradually adapt. Daily temperature range, which  
344 made a better contribution to the PCA than temperature, provides information on the tidal  
345 thermal stress suffered by fauna. However, it is strongly defined by bathymetry, thus would  
346 reflect the sea level rise rather than long-term changes of temperature, it was therefore not  
347 selected.

348 C. Daily salinity range & bathymetry [m] – PC1-PC2: Both factors are accessible at high  
349 frequency, at large scale, and can be measured remotely. They provide a good geographical  
350 description of the estuary, and are strongly affected by climate change, especially by the  
351 global sea level rise, marine intrusion, and changes in the river regime. They are not  
352 significantly correlated ( $R^2 = -0.08$  ns).

353 D. Daily maximum bed shear stress [Pa] & mud content [%] – PC1-PC3: These variables play a  
354 determining role in building an erosion model in the HMS model ( $R^2 = -0.29^{****}$ ). In addition,  
355 the choice relies on close links between the features of the sediment and the responses of  
356 the benthic communities (Andersen et al., 2005).

357 There was no correlation between biological data and any of the environmental factors. Despite the  
 358 high level of correlation and significance between biomass and density ( $R^2 = 0.75^{****}$ ), neither of the  
 359 factors were fully redundant, and the two were consequently analysed in parallel.



360  
 361 *Figure 2: PCA variable correlation plot with the abiotic factors' contributions in bar plots for each axis.*  
 362 *The red dotted line represents the mean contribution for all factors.*

363  
 364 *Table 2 PCA scores for abiotic factors*

Variable	Cos2			Contrib		
	PC1	PC2	PC3	PC1	PC2	PC3
inundation time	0.07	0.67	0.00	1.67	23.10	0.13
current speed	0.72	0.05	0.01	17.82	1.86	0.46
daily maximum current speed	0.79	0.00	0.01	19.65	0.02	0.42
salinity	0.27	0.41	0.03	6.71	14.04	1.23
daily salinity range	0.72	0.09	0.00	17.78	3.02	0.13
temperature	0.07	0.24	0.02	1.83	8.31	1.00
daily temperature range	0.00	0.59	0.01	0.01	20.44	0.52
MES mud	0.37	0.01	0.13	9.18	0.24	5.68
bathymetry	0.01	0.58	0.13	0.28	19.88	5.66

yearly sediment budget	0.00	0.16	0.01	0.00	5.47	0.38
bed shear stress	0.35	0.04	0.40	8.68	1.35	17.99
daily maximum bed shear stress	0.44	0.04	0.16	10.88	1.36	7.25
sediment total concentration	0.10	0.02	0.67	2.51	0.60	30.19
mud content	0.12	0.01	0.64	3.00	0.31	28.96

365

366

### 367 3.3 Description of the Hydro-Morpho-Sedimentary data

368 The selected predictors were observed during the same period and in the same area as the biological  
369 data (Supp. Data 3.3). Generally speaking, all the factors differed significantly in area and period:

370 • Daily maximum current speed [ $\text{m}\cdot\text{s}^{-1}$ ]: the most dynamic area was the channel, with a mean of  
371 1.05 +/- 0.21. The northern upstream and median mudflats were subject to temporal changes  
372 in the distribution of the current in the last period, which had an impact on their global mean  
373 (upstream 0.43 +/- 0.34; median 0.63 +/- 0.3). The south mudflat had same hydrological  
374 conditions than offshore, in between north upstream and median mudflat.

375 • Inundation time [%]: The upstream mudflat, corresponding to upper intertidal areas, had higher  
376 tidal locations than the median mudflat, and shows a decrease in the last period. The south  
377 mudflat had higher inundation time than the north downstream mudflat, the latter being as  
378 subtidal than offshore and channel.

379 • Daily salinity range: This factor varied considerably in space and over time. Offshore and south  
380 mudflat, salinity varied little during the day. Strongly influenced by the river, salinity in the  
381 channel vary of 15-20 during the day, but with a reduction as time went by. The highly  
382 dynamic variations in salinity in the three north mudflats decreased after 2005.

383 • Temperature [ $^{\circ}\text{C}$ ]: A significant global increase in temperature was observed in all areas over  
384 time. The north median mudflat had the highest range, due to its intertidal location.

385 • Mud content [%]: The north upstream mudflat and channel areas were composed with sandy  
386 mud sediment (north upstream mudflat 42 +/- 30; channel 43 +/- 25) with an increase of mud  
387 content for the channel over time. The others are more muddy sands (21 +/- 1), with a  
388 decrease of mud content over time. Mud distribution was heterogeneous in all the areas,  
389 especially the north upstream mudflat.

390 • Daily maximum bed shear stress [ $\text{N}\cdot\text{m}^{-2}$ ]: as reflected in the current speed, the channel had the  
391 highest BSS (3.02 +/- 1.35), while the BSS in the other areas was similar (1.53 +/- 0.65) and  
392 progressively increasing. In the north upstream mudflat, the BSS drop down in the last period  
393 under 1.

394 • Bathymetry [m]: The depth of the channel and offshore were similar, with a mean range of 6.94-  
395 7.95. The north downstream mudflat and the south mudflat were the next deepest areas  
396 (4.16 +/- 0.95), the median mudflat was 1.77 +/- 3.3, and north upstream mudflat was the

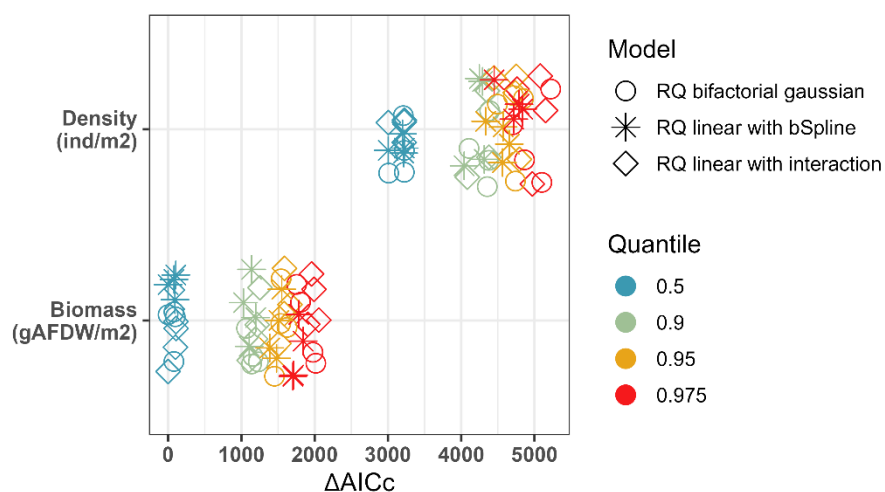
397 shallowest,  $-1.59 \pm 2.63$  (negative bathymetry being above the mean height of sea water)  
398 with again a drop at the last period.

### 399 3.4 Methodology assessment

400 All three calculation response models were used to build SDMs for each abiotic factor set at the  
401 different quantiles chosen. A general comparison of  $\Delta AICc$  scores was undertaken for all the SDMs  
402 computed (Figure 3). The  $\Delta AICc$  scores based on density were significantly higher than those based on  
403 biomass, and the choice of the quantile had a strong impact on the score. For instance, the best scores  
404 were obtained for the biomass SDMs with the 0.5 quantile, which would not help describe the optimum  
405 ecological niche. On average, the BSpline model  $\Delta AICc$  were lower than the others ( $RQ2bsp = 2621 \pm$   
406  $1643$ ,  $RQ2nli = 2717 \pm 1713$ ,  $RQ2int = 2739 \pm 1697$ ). With the same biological response and quantile  
407 (biomass and  $\tau=0.95$ ), the variations between SDM  $\Delta AICc$ s were quite low with respect to total  
408 variability ( $RQ2bsp = 1480 \pm 58$ ,  $RQ2nli = 1529 \pm 49$ ,  $RQ2int = 1575 \pm 39$ ).

409 The predicted/observed plots (Figure 4 shows an example from set A), completed the observations  
410 of  $\Delta AICc$ , i.e.  $RQ2bsp > RQ2nli > RQ2int$  (the regression lines of each quantile were closer to the 1:1  
411 line). However,  $RQ2nli$  performed better than  $RQ2bsp$  at the 95<sup>th</sup> centile, which was defined as the  
412 optimum quantile, i.e. the highest quantile that did not affect model quality, and was hence used for all  
413 subsequent analyses.

414 Based on the range of both predictors under each set, the quantile responses of SDMs were  
415 calculated and illustrated by a surface plot (Figure 5 shows an example from set A, and interactive 3D  
416 plots are provided in Supp. Data 3.4). Although the performance indicators were good, graphically, the  
417  $RQ2bsp$  model showed overfitting which prevented both modelling and prediction. This model was thus  
418 not used for any more analysis.

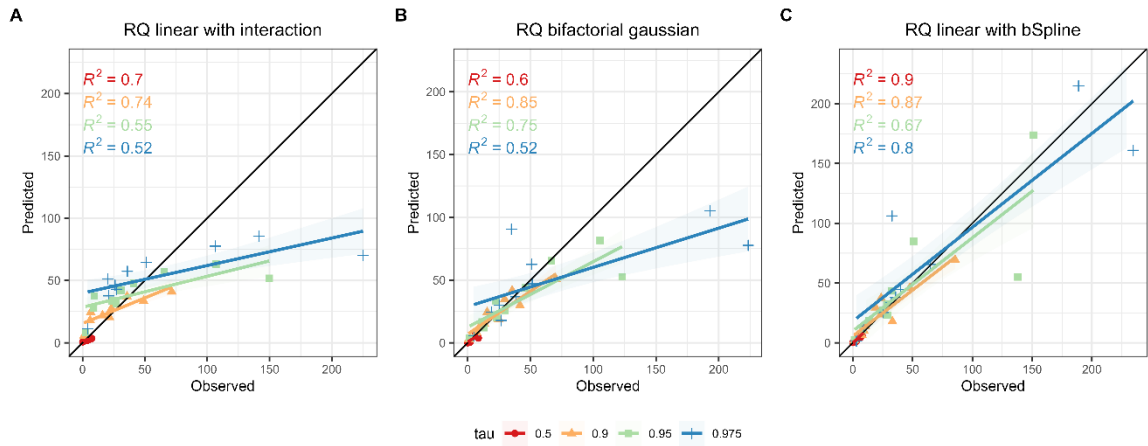


419

420 *Figure 3:  $\Delta AICc$  comparison for all SDMs computed, according to the quantile, the type of model and*  
421 *the response.*

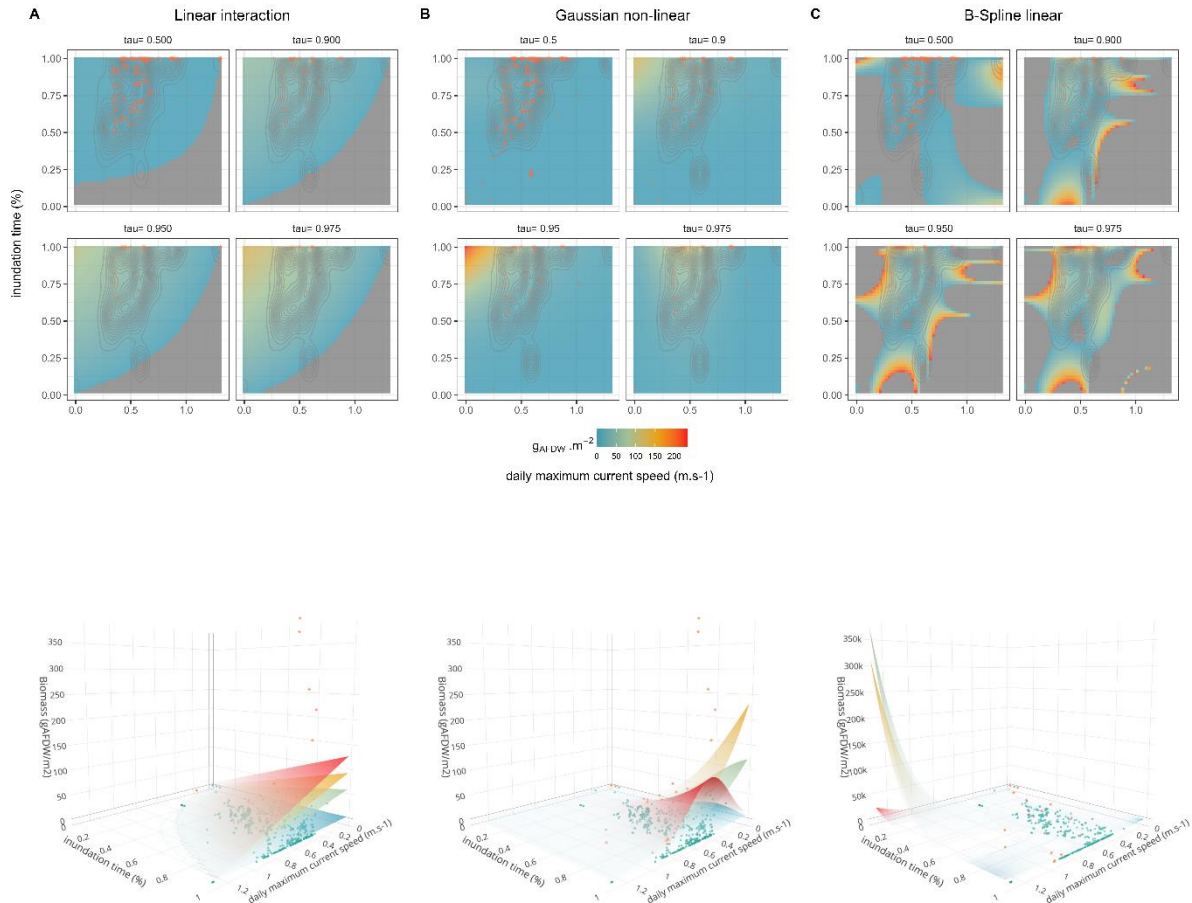


daily maximum current speed (m.s-1) & inundation time (%)



422

423 *Figure 4: Example of modelled vs observed data plotted for each model based on biomass versus*  
 424 *Daily maximum current speed [m.s<sup>-1</sup>] and inundation time [%]. The black line represents the 1:1 ratio,*  
 425 *quantiles 0,5 in red, 0.9 in orange, 0.95 in green and 0.975 in blue.*



426

427 *Figure 5: Examples of SDM surface plots under set A: linear with interaction (A), Gaussian non-linear*  
 428 *(B) and Cubic B-Spline linear (C). The upper panels show for each of the four quantiles: the biological*  
 429 *data observed represented by a contour plot, the model response in colour gradient surface and the*  
 430 *observed data over the model are represented by red stars; the lower panel shows the 3D plots with all*  
 431 *processed quantiles superposed.*



## 432 3.5 Optimal ecological niche

### 433 3.5.1 Comparison of linear and nonlinear Quantile Regression

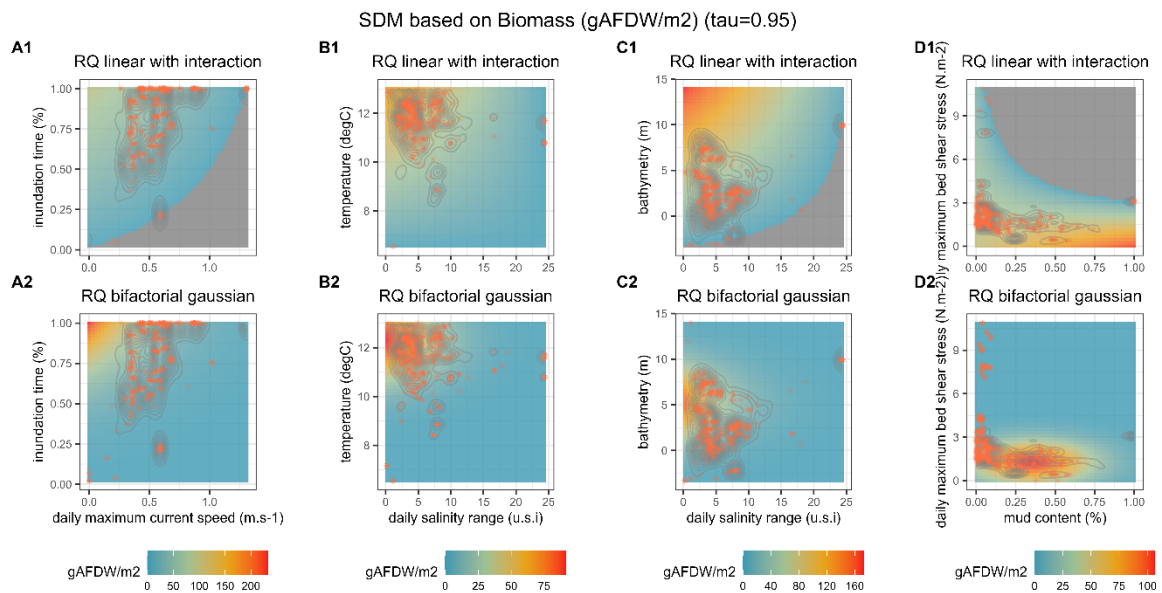
434 The four sets of models with 2 crossed abiotic factors (A, B, C and D, see 3.2 for details) were treated  
435 with one of the two selected models: either linear with interaction, or non-linear with a bifactorial  
436 Gaussian equation, with biomass as biological response (Figure 6, and SDM based on density,  
437 predicted/observed plot and RQ2nli SDMs in 3D graph are available in Supp. Data 3.5.1).

438 A. Daily maximum current speed [ $\text{m}\cdot\text{s}^{-1}$ ] & inundation time [%]: RQ2int optimum was 94.82  
439  $\text{gAFDW}/\text{m}^2$  at  $0 \text{ m}\cdot\text{s}^{-1}$  and 100 %; RQ2nli optimum was  $233 \text{ gAFDW}/\text{m}^2$  at  $0 \text{ m}\cdot\text{s}^{-1}$  and 100  
440 %. The predicted/observed plot shows that RQ2nli performed better than RQ2int. The niche  
441 that was described was a lower intertidal zone with low dynamics, a combination that is rarely  
442 found in the HMS model.

443 B. Daily salinity range & temperature [ $^{\circ}\text{C}$ ]: RQ2int optimum was  $68.96 \text{ gAFDW}/\text{m}^2$  at 0.2 and  
444  $13.01^{\circ}\text{C}$ ; RQ2nli optimum was  $91.35 \text{ gAFDW}/\text{m}^2$  at 0.2 and  $12.35^{\circ}\text{C}$ . The observations fitted  
445 well with the optimum, and the performances of the two models were similar. The ecological  
446 niche corresponding to these models was the mouth of the estuary under temperate  
447 conditions.

448 C. Daily salinity range & bathymetry [m]: RQ2int optimum was  $172.64 \text{ gAFDW}/\text{m}^2$  at 0.2 and  
449  $13.95 \text{ m}$ ; RQ2nli optimum was  $147.6 \text{ gAFDW}/\text{m}^2$  at 0.7 and  $5.14 \text{ m}$ . The observed data were  
450 close to the Gaussian optimum, but not to the linear one, the plot predicted/observed by the  
451 non-linear model was better. With the HMS model, only a few parts of the estuary were less  
452 than 5 m deep, thereby excluding the linear model optimum. With the Gaussian model, the  
453 optimum niche was the end of the mouth of the moderately low intertidal estuary.

454 D. Daily maximum bed shear stress [Pa] & mud content [%]: RQ2int optimum was  $104.58$   
455  $\text{gAFDW}/\text{m}^2$  at 100 % and 0 Pa; RQ2nli optimum was  $106.94 \text{ gAFDW}/\text{m}^2$  at 35 % and 1.33  
456 Pa. The non-linear model optimum was well represented by the observations, in contrast to  
457 the linear, even though the plots predicted/observed by both were good. The linear model  
458 was not in agreement with the knowledge provided by the biological model. The Gaussian  
459 model described a niche of muddy sand in a moderately active hydrodynamic area, likely  
460 undergoing erosion.



461

462 *Figure 6: Sets of quantile regression models with 2 crossed abiotic factors (A,B,C and D see 3.2)*  
 463 *computed with linear model (top row, numbered 1) and non-linear with the Gaussian equation (bottom*  
 464 *row, numbered 2), the observed biological data under the model surface are represented by an isometric*  
 465 *curve, the data over the model are represented by red stars. Each pair has its own range of biomass to*  
 466 *ensure visibility.*

### 467 3.5.2 Non-linear quantile regression with bifactorial Gaussian equation models

468 Overall, the non-linear model performed better than the linear model, and the density-based models  
 469 were generally less relevant than models based on biomass (Figure 3). Thus, the quantile regression  
 470 with bifactorial gaussian (RQ2nli) for biomass was the only model geographically applied and analysed,  
 471 as the normalized suitability index. Each SDM for the RQ2nli model was applied on the HMS model web  
 472 over the estuary, for each period (Figure 7, density in Supp. Data 3.5.2.1). The suitability index is given  
 473 per period and area (Figure 8, density in Supp. Data 3.5.2.2, and suitability index compared to the two  
 474 abiotic factor plot in Supp. Data 3.5.2.3), in detail:

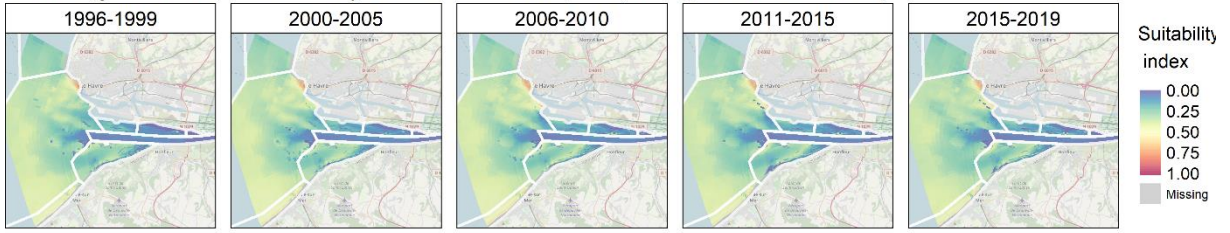
475 A. Daily maximum current speed [m.s<sup>-1</sup>] & inundation time [%]: The maps (Figure 7) showed that  
 476 the channel and north mudflats were the least favourable areas, the south mudflats and  
 477 offshore were more appropriate, but few locations were really optimum. The suitability index  
 478 (Figure 8), which ranged from 0.1 to 0.3 and was generally stable, confirmed that the most  
 479 suitable area was offshore, followed by south mudflat. The suitability of the north median  
 480 and upstream mudflats improved after 2005, when they became better than the channel.

481 B. Daily salinity range & temperature [°C]: The salinity part of the model had a noticeable effect  
 482 on the result of the model (Figure 7), with a clear reduction in biomass in the river and its  
 483 ETM area. The closer the estuary entrance to the sea, the higher the model, the offshore  
 484 area having a clear advantage that increased from 2005 on. The suitability index (Figure 8)  
 485 ranged from 0 to 0.7. The three north mudflats underwent a significant increase during the  
 486 first three periods. Offshore and south mudflats were similar and the most suitable, joined by  
 487 north downstream mudflat at the last 3 periods, the channel being the least suitable area.

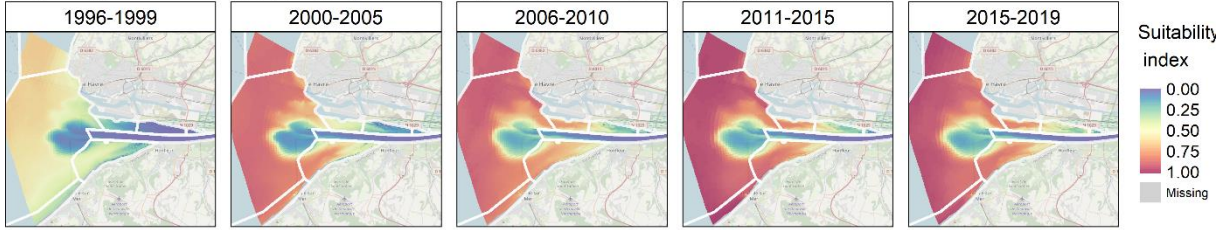
488 C. Daily salinity range & bathymetry [m]: The optima for this model were clearly located on the  
489 south mudflat (Figure 7), results linked to the bathymetry. Offshore, a spot was high in the  
490 period 1996-1999 caused by dumping material dredged from the channel that was  
491 subsequently progressively smoothed. Suitability index was less than 0.5, the south mudflat  
492 being the best (Figure 8). Apart from the north median and downstream mudflats which  
493 increased over the first three periods, the indexes for each area remained steady.

494 D. Daily maximum bed shear stress [Pa] & mud content [%]: This model result was very patchy  
495 at the scale of the estuary due to the equally patchy distribution of mud (Figure 7). This  
496 identified a channel with high biomass potential, which did not agree with expert knowledge.  
497 There was also an area with high biomass around the borders of the ETM area offshore  
498 which decreased over time, also due to the reduced mud content. Suitability ranged from  
499 0.25 to 0.75 (Figure 8), with a complex pattern. The suitability of the channel, offshore, south  
500 mudflat and north downstream mudflat decreased after 2005, while the suitability of north  
501 upstream and median mudflats improved.

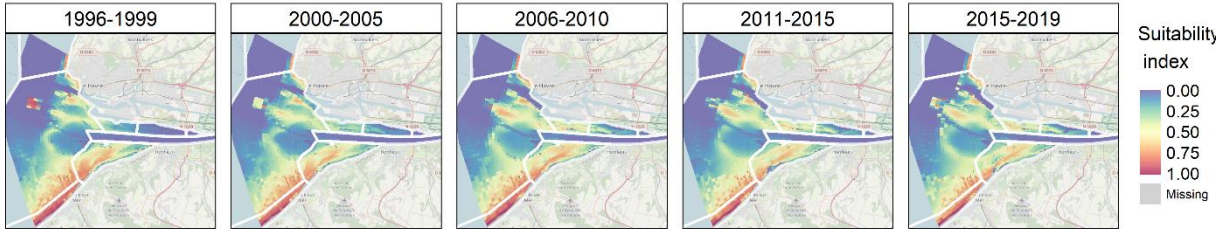
RQ2nli (gAFDW/m<sup>2</sup>) t0.950 - daily maximum current speed (m.s-1) \* inundation time (%)



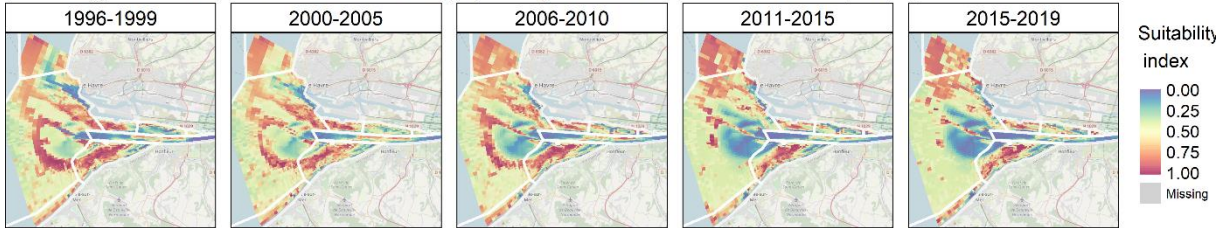
RQ2nli (gAFDW/m<sup>2</sup>) t0.950 - daily salinity range (u.s.i) \* temperature (degC)



RQ2nli (gAFDW/m<sup>2</sup>) t0.950 - daily salinity range (u.s.i) \* bathymetry (m)



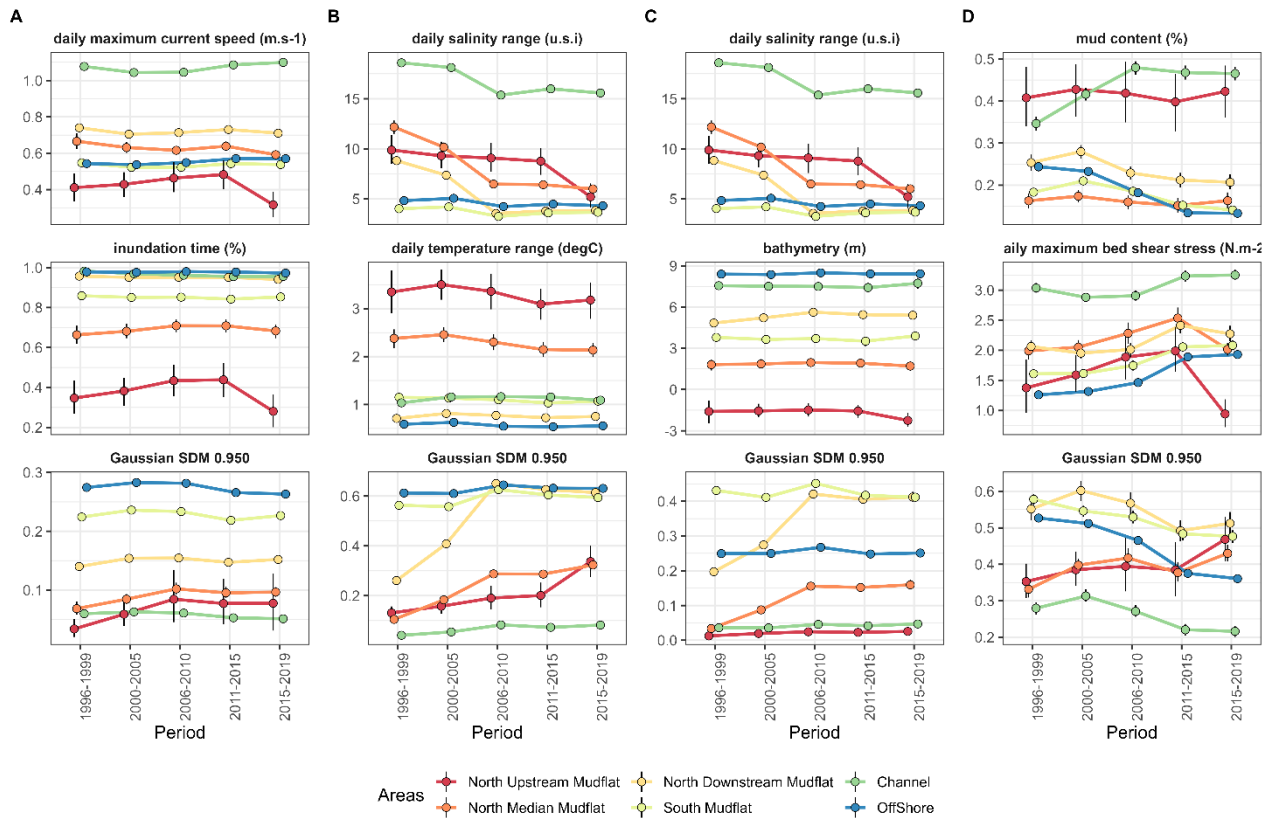
RQ2nli (gAFDW/m<sup>2</sup>) t0.950 - mud content (%) \* daily maximum bed shear stress (N.m-2)



502

503

Figure 7: SDM models suitability index applied on the Seine estuary over the five periods.



504

505 *Figure 8: Abiotic factors and resulting SDM suitability index per period and per area for all SDM*  
 506 *models with a 95% confidence interval.*

507 **4 Discussion**

508 **4.1 Assessment of the methodology**

509 The quality of a SDM depends first and foremost on the reliability of the input data. The biological  
 510 data used in this study comes from community monitoring programmes with a continuity of practices,  
 511 and even of operators, which makes it possible to process data together over such a long period of time.  
 512 Physical gradients condition complex interactions with fauna in estuaries (Chapman et al., 2010;  
 513 Herman et al., 2001). However, community self-organisation also takes place at several overlapping  
 514 spatial scales, strongly expressed by tidal constraints, where micro-scale organisations are able to  
 515 create micro-climates (“shelters”) that can accommodate very high densities of fauna (Ettema and  
 516 Wardle, 2002; Le Hir and Hily, 2005; Thrush et al., 2005; Underwood and Chapman, 1996). The abiotic  
 517 field data, synchronous with the biological data, are more susceptible to highlight very small atypical  
 518 habitats than macro-spatial trends. The use of a hydro-morpho-sedimentary model therefore makes it  
 519 possible to better describe the overall “smoothed” environment. However, even if hydrological  
 520 measurements and models are becoming increasingly reliable, modelling of the seabed and sediment  
 521 transport still needs to be improved (Grasso et al., 2018). The complexity of an intertidal environment  
 522 with its locally very different micro-habitats is difficult to portray on the scale of a model with a cell size  
 523 of, at best, 100 m.

524 In order to align the biological data with the abiotic data, the latter were summarised at their annual  
525 median. With the exception of temperature, and to a lesser extent the daily maximum bed shear stress,  
526 the seasonal medians (winter from October to March and summer from April to September) do not differ  
527 significantly from the annual average. Nevertheless, the history of extreme events such as heat waves  
528 or storms is smoothed out, which is an obvious limitation of the study, as a punctual extreme event can  
529 lead to drastic changes in community succession initiated by a long-term change in physical conditions  
530 (Baltar et al., 2019).

531 SDMs can be constructed using an unlimited set of abiotic variables to define an ecological niche.  
532 However, an n-dimensional space is difficult to analyse from an ecological point of view as would be  
533 recommended (Austin, 2002). On the contrary, a single SDM predictor is possible, but it represents a  
534 risk of oversimplification that would result in an unreliable model. The choice of using two predictors,  
535 selected via a PCA analysis, makes it possible to further refine the description of an environment, and  
536 visualize the niche to confront it to ecological knowledge and intrinsic ecophysiological processes. In  
537 addition, we chose to present four SDMs, because it seemed reasonable to show different combinations  
538 of selected factors, rather than describing only one « supposed » best solution. Our sets have been  
539 designed to assess the impacts of different climate change effects on an estuary, while ensuring that  
540 the models can also be applied to other estuarine environments.

541 The quantile regression used in this study is interesting in that the biological response can be better  
542 modelled by two abiotic factors, even if there are other limiting factors. The abiotic data from HMS  
543 models can be used to describe complex patterns between the main physical factors, but at the very  
544 least they do not reflect the chemical variations (possible contamination) or biological interactions  
545 (competitive pressure, for example) involved in determining the dynamics of a population. Quantile  
546 regression at a high quantile level therefore makes it possible to limit the attenuating effects of factors  
547 not taken into account on the biological response.

548 There are experimental studies on the biological response to ranges of variation in temperature,  
549 salinity or even pH, which can provide a better understanding of the mechanistic basis of metabolisms  
550 on organism performance (Hale et al., 2011; Łapucki and Normant, 2008; Lemasson et al., 2017;  
551 Madeira et al., 2021; Medeiros et al., 2020; Ong et al., 2017; Peteiro et al., 2018). However, this type of  
552 approach cannot be applied to incorporate the effects of other physical factors. Exploratory methods  
553 based on long series of observations, such as those proposed here, remain one good method for  
554 integrating all the processes responsible for changes in habitability for populations such as cockles,  
555 without any preconceived ideas. It is known that physical stresses play a very significant role in the  
556 population dynamics of this species. Our study may enable us to make better progress in understanding  
557 the possible evolution of species on a multifactorial basis, before going further and validating new  
558 hypotheses through comparisons with other ecosystems or new experimental work in macrocosms, for  
559 example, enabling us to better identify the effects of all the factors.

560 This study compared a linear quantile regression to a non-linear quantile regression based on a bell-  
561 shaped curve and a B-Spline model. Considering only the AIC and the predicted/observed graphs, the  
562 linear model with B-Spline of the 3<sup>rd</sup> degree can appear efficient. However, even if the three calculation



563 modes did provide a solution, the Gaussian model was the only adequate on an ecological point of view,  
564 that could truly rely upon specific traits. The choice of the observation quantile is a subject of discussion,  
565 as the SDMs produced very different results from one quantile to another. In this study, we chose to  
566 limit the number of quantiles to enable clear visualization of the models, but it is also possible to push  
567 the analysis to the point of looking for the highest quantile that still performs well. Yet, the aim of this  
568 study was to define the most favourable HMS conditions for the development of a species, not  
569 necessarily the niche representing the most exceptional circumstances. In fact, the very high quantiles  
570 will correspond to the niche that accounts for the biological observations resulting from the patchiness  
571 distribution of species.

## 572 4.2 Optimal ecological niches for cockles

573 When we compared the four sets of crossed factors (A: daily maximum current speed & inundation  
574 time, B: daily salinity range & temperature, C: daily salinity range & bathymetry, D: daily maximum bed  
575 shear stress & mud content), the quantile regression adjusted models revealed differences between  
576 them linked to the choice of predictors that led to different levels of expected biomass. Therefore, as the  
577 modelled biomass represent a carrying capacity that are difficult to observe, it was decided to compare  
578 the standardised results for each SDM.

579 The combination daily maximum current speed & inundation time (A) was based on the  
580 hydrodynamics generated by the meeting of the two masses of fresh and marine water under the effect  
581 of the tides and the fluvial regime (PCA1) and the morphology of the estuary, which generates shallow  
582 and intertidal areas (PCA2). Under these conditions, salinity increases with water depth, as it represents  
583 the upstream-downstream gradient of the estuary, and the greater the hydrodynamic conditions, the  
584 greater the mixing between fresh and marine waters. On the other hand, shallow waters follow day-to-  
585 day temperature variations more dynamically. The optimum of this model therefore represents a low  
586 intertidal marine niche, without intense variation in salinity and temperature. For the daily maximum  
587 current speed, this model shows an interesting variation in the niche between the 95<sup>th</sup> and 97.5<sup>th</sup>  
588 quantiles (Figure 5): the optimum of the 97.5<sup>th</sup> percentile (0.5 m.s<sup>-1</sup>) is better represented by the  
589 observed data than the 95<sup>th</sup>, while the quantile plot shows a better performance of the 95<sup>th</sup>. 97.5<sup>th</sup>  
590 percentile shows that the cockle would have interest of having some hydrodynamics in their habitat.

591 Using inundation time rather than bathymetry as an abiotic descriptor was a better way to reflect the  
592 type of tidal of the estuary, in this case macro-tidal. The tide affects the feeding periods of the benthic  
593 fauna and the periods when they are accessible to predators, but also the daily hydrological conditions,  
594 as shown in set A. For their SDM, Cozzoli et al. used the same set of parameters with a higher centile,  
595 97.5<sup>th</sup>, applied to a data set located in the Oosterschelde estuary, and obtained different results (Cozzoli  
596 et al., 2014). They observed that the optimum was found in a medium intertidal zone with a maximum  
597 current of 0.5 m.s<sup>-1</sup>. It should be noted that the current range was wider than the range we obtained for  
598 the SDMs in this study.

599 The model using daily salinity range & temperature (B) is based on the same aspects of the estuary,  
600 only using the physico-chemical aspects of the water. The optimum niche for this model is low variations



601 of salinity, hence the mouth of the estuary since the model is not calculated in its fluvial part. The  
602 optimum temperature is temperate (12.35°C) meaning that at upper temperature, the suitability  
603 decreases. This optimum corresponds to a little warmer than the global temperature found in the  
604 estuary, without the seasonal variability ( $12.15 \pm 4.75^\circ\text{C}$ ), meaning that the cockle population is  
605 acclimated to the normal conditions found in their habitat. The optimum niche based on daily salinity  
606 range & bathymetry (C) is the same as the previous model regarding the salinity parameter, and the  
607 optimum bathymetry (5.14 m) corresponds to the low intertidal areas, almost subtidal, as shown in SDM  
608 A. This model is therefore aligned with SDM A describing the low intertidal mouth of estuary.

609 The model based on daily maximum bed shear stress & mud content (D) represents the  
610 hydrodynamics of the estuary (PC1) like the other 3 models, but adding another piece of information  
611 with the sediment composition of the estuary bed (PC3). The optimal daily maximum bed shear stress,  
612 corresponding to daily maximum current lower to  $1 \text{ m}\cdot\text{s}^{-1}$ , is likely to generate erosion (1.33 Pa), but on  
613 the contrary to the model A, the absence of hydrodynamics is not the optimum, as would suggest the  
614 97.5<sup>th</sup> quantile for model A. From a sedimentary point of view, the niche describes a muddy sand, which  
615 corresponds to what we know about the species.

616 Overall, when considering all bifactorial Gaussian quantile regression models, the best conditions for  
617 cockles appear to be in lower intertidal marine areas, with temperate and low dynamic waters, settled  
618 in muddy sand sediment. This description is in agreement with habitat EUNIS 2008 A2.242:  
619 *Cerastoderma edule* and polychaetes in littoral muddy sand (Tillin and Tyler-Walters, 2016; Tyler-  
620 Walters, 2007). Observations by Boyden and Russell in cockle habitats were similar, although these  
621 authors concluded that tidal flow was more determinant than salinity, the latter being an indirect indicator  
622 of the former in brackish waters, and that cockles were unable to settle in still water (Boyden and Russell,  
623 1972). SDM A was more tolerant to still water at the 95<sup>th</sup> centile, but in agreement at the 97.5<sup>th</sup> centile.

### 624 4.3 A tool for ecosystem management

625 The SDM is a useful tool for environmental management, able to highlight any spatio-temporal  
626 differences in a given territory and makes it possible to monitor changes in physical parameters that are  
627 more accessible than data on species communities. In the present study, we chose to display the main  
628 results of SDM in the form of suitability index, based on simple normalization, to characterise the  
629 differences between two areas and between two periods. By making the SDM dimensionless, the index  
630 prevents interpretation of the result as the real amount of biomass. Still, as SDMs are linked to HMS  
631 variables, the suitability index is a good indicator of potential levers to cope with changes in suitability,  
632 particularly due to human activities, as well as with the effects of the global climate change.

633 When considering spatial application of the niches, an area under high human influence like the  
634 Seine estuary has HMS conditions that can be considered anomalies in the functioning of an estuary.  
635 The Seine channel is a major shipping route for the French economy and is therefore regularly dredged,  
636 and the sediment that is removed is dumped offshore. This artificial sediment transport not only modifies  
637 the bathymetry, but also the hydrological dynamics. As a result, certain areas of the estuary were applied  
638 but not included in the analysis of the results of the niche application: the Côte Fleurie and Octeville, the

639 port and the beach of Le Havre are areas heavily disturbed by human activities. In addition, Cap Hève,  
640 south of the Octeville area, is an area with a bedrock substrate in which cockles cannot be present. The  
641 spatial application of the model must therefore be limited to areas where human impact remains  
642 reasonable. For this reason, the analysis of the suitability index focuses on the mudflats, with the channel  
643 and the offshore area as points of comparison.

644 As expected, all the suitability indexes show low values for the channel. North upstream and median  
645 mudflats are generally of the same range of suitability, quite low but slightly improving with time. North  
646 upstream mudflat shows a high range of variability, due to different conditions in the area. North  
647 downstream mudflat has an improvement of suitability, after 2005, to end at the same level than the  
648 south mudflat, except for SDM A, where it remains lower. The more suitable area was the south mudflat  
649 for all SDM, often at the same level as the offshore (except for SDM C). The gradient from upstream to  
650 downstream is quite visible on all SDMs.

651 If we compare the temporal evolution of the index for the different zones with the evolution of the  
652 abiotic factors, we can see that the evolution of the daily salinity range is the parameter that has the  
653 greatest impact on the intertidal zones. For the northern upstream and median mudflats, the variation in  
654 salinity decreased after 2005, i.e. after the Port 2000 project, which increased the channelling of the  
655 estuary and therefore reduced the communication between the river and the tidal flats along its banks.  
656 In addition, the global temperature shows a significant increase over the years, especially in intertidal  
657 areas, which led to more suitability in SDM B. This model is the only taking into account the direct effect  
658 of temperature increases due to climate change, that is already visible in the period of data available.  
659 This model is the most sensitive to heat waves and presents a risk if extrapolated outside the model's  
660 definition range, as it does not take into account the acclimatisation of species in the niche, or at least  
661 the rate of acclimatisation in relation to the rate of warming of the waters of the estuary.

662 Although SDMs define optimum environments, they do not account for bioturbation or food-web  
663 processes, for example. Cockles are known eco-engineers which can modify their environment,  
664 especially sediment content (Donadi et al., 2014, 2013). They alter their habitat to obtain better  
665 conditions (Li et al., 2017), and interact strongly with the microphytobenthos, creating biofilms that alter  
666 sediment erosion properties (Eriksson et al., 2017; Ubertini et al., 2012). Those effects were assumed  
667 to be included in the variability of the response in all SDMs, but the processes themselves are inevitably  
668 hidden. Many of the processes involving fauna, flora and habitats have feedback loop effects, especially  
669 bioturbation, which have not yet been incorporated in HMS models, and the models thus fail to truly  
670 represent the mechanisms behind the species distribution. Even if self-organisation processes related  
671 to ecosystem engineering are totally masked by the SDM approach as direct factors, they must interfere  
672 and the best optimal habitat is in fact the one where self-organisation and other positive feedbacks  
673 [biogeochemical regulation by bioturbation processes and positive feedbacks with microphytobenthos  
674 production (Cade et al., 2005)]. This hypothesis could be tested experimentally to better refine the  
675 definition of optimal habitats.

676 A further limitation of this study is the use of a single species, *Cerastoderma edule*, but our method  
677 can be used for other abundant species present in the estuary, particularly species that are known to

678 share the same habitats, such as *Macoma balthica*, *Scrobicularia plana*, *Hediste diversicolor*,  
679 *Corophium volutator* and *Peringia ulvae* (EUNIS habitat A2.24 : Polychaete/bivalve-dominated muddy  
680 sand shores (A2.241/MA5251, A2.242/MA5252, A2.243/MA5253) and A2.31 : Polychaete/bivalve-  
681 dominated mid estuarine mud shores (A2.312/MA6224, A2.313/MA6225) (European Environment  
682 Agency, 2023)). To go still further, it would be advantageous to develop a community scale indicator,  
683 based on the life traits, functional traits or ecosystem services the macrofauna can provide, as one  
684 species could progressively be replaced by another species that is equivalent from some points of view.  
685 Such upscaling would be important before applying the SDM to projections on a future representing the  
686 local effects of global climate change.

## 687 5 Conclusion

688 The development of accessible mathematical and statistical tools has considerably broadened the  
689 methodologies to build SDMs, and have been applied to different environments in dissimilar ways. Due  
690 to their complex structure and strong gradients, estuarine environments can benefit from the extraction  
691 of physical descriptors from models of water and sediment transports and the quantile regression  
692 approach. This tool helps define the areas that are suitable for targeted species based on a long time  
693 series data. However, the choice of environmental factors plays a decisive role in the result, and several  
694 models should be combined to obtain an overview of how the target fauna interacts with its environment.  
695 In this study, a suitability index is proposed as an indicator of the habitability of areas, based on a  
696 representative species, the cockle, but the index could be developed, as a prospect, into a community-  
697 based index, in order to take better account of the ecosystem services that the benthic macrofauna  
698 provides to the estuary.

## 699 Acknowledgements

700 The authors thank Francesco Cozzoli and Tjeerd Bouma for their guidance and insights on the  
701 MELTING POTES project; Brian Cade for his precious help on quantile regression; The GIP Seine Aval,  
702 the Maison de l'Estuaire, the Cellule du Suivi du Littoral Normand and the Grand Port Maritime du Havre  
703 for the biological datasets; IFREMER for the Mars3D model dataset. The authors acknowledge  
704 anonymous reviewers for their valuable comments and suggestions.

## 705 Funding

706 This research was supported by the *Region Normandie* (A. Lehuen's PhD) and by the *Office Français*  
707 *pour la Biodiversité* (the MELTING POTES project).

## 708 CRediT author statement

709 A. Lehuen: Conceptualization, Methodology, Formal analysis, Writing - Original Draft, Funding  
710 acquisition ; C. Dancie: Resources, Data Curation, Writing - Review & Editing ; F. Grasso: Resources,  
711 Data Curation, Writing - Review & Editing; F. Orvain: Conceptualization, Methodology, Validation,  
712 Resources, Writing - Review & Editing, Supervision, Project administration, Funding acquisition

## 713 References

- 714 Akaike, H., 1974. A new look at the statistical model identification. *IEEE Trans. Autom. Control* 19, 716–  
715 723. <https://doi.org/10.1109/TAC.1974.1100705>
- 716 Andersen, T.J., Lund-Hansen, L.C., Pejrup, M., Jensen, K.T., Mouritsen, K.N., 2005. Biologically  
717 induced differences in erodibility and aggregation of subtidal and intertidal sediments: a possible  
718 cause for seasonal changes in sediment deposition. *J. Mar. Syst.* 55, 123–138.  
719 <https://doi.org/10.1016/j.jmarsys.2004.09.004>
- 720 Anderson, M.J., 2008. Animal-sediment relationships re-visited: Characterising species' distributions  
721 along an environmental gradient using canonical analysis and quantile regression splines. *J.*  
722 *Exp. Mar. Biol. Ecol.* 366, 16–27. <https://doi.org/10.1016/j.jembe.2008.07.006>
- 723 Aulert, C., Provost, P., Bessineton, C., Dutilleul, C., 2009. Les mesures compensatoires et  
724 d'accompagnement Port 2000 : retour d'expériences. *Ingénieries* 55–72.
- 725 Austin, M., 2007. Species distribution models and ecological theory: A critical assessment and some  
726 possible new approaches. *Ecol. Model.* 200, 1–19.  
727 <https://doi.org/10.1016/j.ecolmodel.2006.07.005>
- 728 Austin, M.P., 2002. Spatial prediction of species distribution: an interface between ecological theory and  
729 statistical modelling. *Ecol. Model.* 157, 101–118. [https://doi.org/10.1016/S0304-3800\(02\)00205-3](https://doi.org/10.1016/S0304-3800(02)00205-3)
- 731 Bacouillard, L., Baux, N., Dauvin, J.-C., Desroy, N., Geiger, K.J., Gentil, F., Thiébaud, É., 2020. Long-  
732 term spatio-temporal changes of the muddy fine sand benthic community of the Bay of Seine  
733 (eastern English Channel). *Mar. Environ. Res.* 161, 105062.  
734 <https://doi.org/10.1016/j.marenvres.2020.105062>
- 735 Baffreau, A., Pezy, J.-P., Dancie, C., Chouquet, B., Hacquebart, P., Poisson, E., Foveau, A., Joncourt,  
736 Y., Duhamel, S., Navon, M., Marmin, S., Dauvin, J.-C., 2017. Mapping benthic communities: An  
737 indispensable tool for the preservation and management of the eco-socio-system in the Bay of  
738 Seine. *Reg. Stud. Mar. Sci.* 9, 162–173. <https://doi.org/10.1016/j.rsma.2016.12.005>

739 Baltar, F., Bayer, B., Bednarsek, N., Deppeler, S., Escribano, R., Gonzalez, C.E., Hansman, R.L.,  
740 Mishra, R.K., Moran, M.A., Repeta, D.J., Robinson, C., Sintes, E., Tamburini, C., Valentin, L.E.,  
741 Herndl, G.J., 2019. Towards Integrating Evolution, Metabolism, and Climate Change Studies of  
742 Marine Ecosystems. *Trends Ecol. Evol.* 34, 1022–1033.  
743 <https://doi.org/10.1016/j.tree.2019.07.003>

744 Beck, M.W., Heck, K.L., Able, K.W., Childers, D.L., Eggleston, D.B., Gillanders, B.M., Halpern, B., Hays,  
745 C.G., Hoshino, K., Minello, T.J., Orth, R.J., Sheridan, P.F., Weinstein, M.P., 2001. The  
746 Identification, Conservation, and Management of Estuarine and Marine Nurseries for Fish and  
747 Invertebrates. *BioScience* 51, 633. [https://doi.org/10.1641/0006-  
748 3568\(2001\)051\[0633:TICAMO\]2.0.CO;2](https://doi.org/10.1641/0006-3568(2001)051[0633:TICAMO]2.0.CO;2)

749 Boesch, D.F., Turner, R.E., 1984. Dependence of fishery species on salt marshes: The role of food and  
750 refuge. *Estuaries* 7, 460–468. <https://doi.org/10.2307/1351627>

751 Bolker, B.M., Brooks, M.E., Clark, C.J., Geange, S.W., Poulsen, J.R., Stevens, M.H.H., White, J.-S.S.,  
752 2009. Generalized linear mixed models: a practical guide for ecology and evolution. *Trends*  
753 *Ecol. Evol.* 24, 127–135. <https://doi.org/10.1016/j.tree.2008.10.008>

754 Boyden, C.R., Russell, P.J.C., 1972. The Distribution and Habitat Range of the Brackish Water Cockle  
755 (*Cardium (Cerastoderma) glaucum*) in the British Isles. *J. Anim. Ecol.* 41, 719.  
756 <https://doi.org/10.2307/3205>

757 Brown, J.H., Stevens, G.C., Kaufman, D.M., 1996. The Geographic Range: Size, Shape, Boundaries,  
758 and Internal Structure. *Annu. Rev. Ecol. Syst.* 27, 597–623. <https://doi.org/10.2307/2097247>

759 Cade, B.S., Noon, B.R., 2003. A gentle introduction to quantile regression for ecologists. *Front. Ecol.*  
760 *Environ.* 1, 412–420. [https://doi.org/10.1890/1540-9295\(2003\)001\[0412:AGITQR\]2.0.CO;2](https://doi.org/10.1890/1540-9295(2003)001[0412:AGITQR]2.0.CO;2)

761 Cade, B.S., Noon, B.R., Flather, C.H., 2005. Quantile regression reveals hidden bias and uncertainty in  
762 habitat models. *Ecology* 86, 786–800. <https://doi.org/10.1890/04-0785>

763 Cade, B.S., Terrell, J.W., Schroeder, R.L., 1999. Estimating effects of limiting factors with regression  
764 quantiles 80, 13.

765 Chapman, M., Tolhurst, T., Murphy, R., Underwood, A., 2010. Complex and inconsistent patterns of  
766 variation in benthos, micro-algae and sediment over multiple spatial scales. *Mar. Ecol. Prog.*  
767 *Ser.* 398, 33–47. <https://doi.org/10.3354/meps08328>

768 Cozzoli, F., Bouma, T., Ysebaert, T., Herman, aPMJ, 2013. Application of non-linear quantile regression  
769 to macrozoobenthic species distribution modelling: comparing two contrasting basins. *Mar.*  
770 *Ecol. Prog. Ser.* 475, 119–133. <https://doi.org/10.3354/meps10112>

771 Cozzoli, F., Eelkema, M., Bouma, T.J., Ysebaert, T., Escaravage, V., Herman, P.M.J., 2014. A Mixed  
772 Modeling Approach to Predict the Effect of Environmental Modification on Species Distributions.  
773 *PLoS ONE* 9, e89131. <https://doi.org/10.1371/journal.pone.0089131>

- 774 Cozzoli, F., Smolders, S., Eelkema, M., Ysebaert, T., Escaravage, V., Temmerman, S., Meire, P.,  
775 Herman, P.M.J., Bouma, T.J., 2017. A modeling approach to assess coastal management  
776 effects on benthic habitat quality: A case study on coastal defense and navigability. *Estuar.  
777 Coast. Shelf Sci.* 184, 67–82. <https://doi.org/10.1016/j.ecss.2016.10.043>
- 778 Crossland, C.J., Baird, D., Ducrotoy, J.-P., Lindeboom, H., Buddemeier, R.W., Dennison, W.C.,  
779 Maxwell, B.A., Smith, S.V., Swaney, D.P., 2005. The Coastal Zone — a Domain of Global  
780 Interactions, in: Crossland, C.J., Kremer, H.H., Lindeboom, H.J., Marshall Crossland, J.I., Le  
781 Tissier, M.D.A. (Eds.), *Coastal Fluxes in the Anthropocene*, Global Change — The IGBP Series.  
782 Springer Berlin Heidelberg, Berlin, Heidelberg, pp. 1–37. [https://doi.org/10.1007/3-540-27851-  
783 6\\_1](https://doi.org/10.1007/3-540-27851-6_1)
- 784 Dauvin, J.-C., 2015. History of benthic research in the English Channel: From general patterns of  
785 communities to habitat mosaic description. *J. Sea Res., MeshAtlantic: Mapping Atlantic Area  
786 Seabed Habitats for Better Marine Management* 100, 32–45.  
787 <https://doi.org/10.1016/j.seares.2014.11.005>
- 788 Dauvin, J.C., Ruellet, T., Desroy, N., Janson, A.-L., 2006. Indicateurs benthiques de l'état des  
789 peuplements benthiques de l'estuaire marin et moyen et de la partie orientale de la Baie de  
790 Seine. *Rapport scientifique Seine-Aval 3. Theme 3: Tableau de bord et indicateurs  
791 opérationnels*. GIP Seine Aval.
- 792 Degraer, S., Verfaillie, E., Willems, W., Adriaens, E., Vincx, M., Van Lancker, V., 2008. Habitat suitability  
793 modelling as a mapping tool for macrobenthic communities: An example from the Belgian part  
794 of the North Sea. *Cont. Shelf Res.* 28, 369–379. <https://doi.org/10.1016/j.csr.2007.09.001>
- 795 Donadi, S., van der Zee, E.M., van der Heide, T., Weerman, E.J., Piersma, T., van de Koppel, J., Olf, H.,  
796 Bartelds, M., van Gerwen, I., Eriksson, B.K., 2014. The bivalve loop: Intra-specific facilitation  
797 in burrowing cockles through habitat modification. *J. Exp. Mar. Biol. Ecol.* 461, 44–52.  
798 <https://doi.org/10.1016/j.jembe.2014.07.019>
- 799 Donadi, S., Westra, J., Weerman, E.J., van der Heide, T., van der Zee, E.M., van de Koppel, J., Olf, H.,  
800 Piersma, T., van der Veer, H.W., Eriksson, B.K., 2013. Non-trophic Interactions Control Benthic  
801 Producers on Intertidal Flats. *Ecosystems* 16, 1325–1335. [https://doi.org/10.1007/s10021-013-  
802 9686-8](https://doi.org/10.1007/s10021-013-9686-8)
- 803 Dubois, S., Marin-Léal, J.C., Ropert, M., Lefebvre, S., 2007. Effects of oyster farming on macrofaunal  
804 assemblages associated with *Lanice conchilega* tubeworm populations: A trophic analysis using  
805 natural stable isotopes. *Aquaculture* 271, 336–349.  
806 <https://doi.org/10.1016/j.aquaculture.2007.03.023>
- 807 Elith, J., Leathwick, J.R., 2009. Species Distribution Models: Ecological Explanation and Prediction  
808 Across Space and Time. *Annu. Rev. Ecol. Evol. Syst.* 40, 677–697.  
809 <https://doi.org/10.1146/annurev.ecolsys.110308.120159>

810 Eriksson, B.K., Westra, J., van Gerwen, I., Weerman, E., van der Zee, E., van der Heide, T., van de  
811 Koppel, J., Olf, H., Piersma, T., Donadi, S., 2017. Facilitation by ecosystem engineers  
812 enhances nutrient effects in an intertidal system. *Ecosphere* 8, e02051.  
813 <https://doi.org/10.1002/ecs2.2051>

814 Ettema, C.H., Wardle, D.A., 2002. Spatial soil ecology. *Trends Ecol. Evol.* 17, 177–183.  
815 [https://doi.org/10.1016/S0169-5347\(02\)02496-5](https://doi.org/10.1016/S0169-5347(02)02496-5)

816 European Environment Agency, 2023. EUNIS -EUNIS habitat types hierarchical view - revised groups  
817 [WWW Document]. URL <https://eunis.eea.europa.eu/habitats-code-browser-revised.jsp>  
818 (accessed 8.2.23).

819 Franklin, J., 2010. Mapping Species Distributions: Spatial Inference and Prediction, Ecology,  
820 Biodiversity and Conservation. Cambridge University Press, Cambridge.  
821 <https://doi.org/10.1017/CBO9780511810602>

822 Goberville, E., Beaugrand, G., Sautour, B., Tréguer, P., Somlit, T., 2010. Climate-driven changes in  
823 coastal marine systems of western Europe. *Mar. Ecol. Prog. Ser.* 408, 129–147.  
824 <https://doi.org/10.3354/meps08564>

825 Gosling, E.M., 2003. Bivalve molluscs: biology, ecology, and culture, Fishing News Books. ed. Blackwell  
826 Publishing, Oxford ; Malden, MA.

827 Grassle, F.J., 2013. Marine Ecosystems, in: Encyclopedia of Biodiversity. Elsevier, pp. 45–55.  
828 <https://doi.org/10.1016/B978-0-12-384719-5.00290-2>

829 Grasso, F., Bismuth, E., Verney, R., 2021. Unraveling the impacts of meteorological and anthropogenic  
830 changes on sediment fluxes along an estuary-sea continuum. *Sci. Rep.* 11, 20230.  
831 <https://doi.org/10.1038/s41598-021-99502-7>

832 Grasso, F., Bismuth, E., Verney, R., 2019. ARES hindcast [WWW Document]. Sextant. URL  
833 <https://sextant.ifremer.fr/geonetwork/srv/api/records/8f5ec053-52c8-4120-b031-4e4b6168ff29>  
834 (accessed 5.13.23).

835 Grasso, F., Le Hir, P., 2019. Influence of morphological changes on suspended sediment dynamics in  
836 a macrotidal estuary: diachronic analysis in the Seine Estuary (France) from 1960 to 2010.  
837 *Ocean Dyn.* 69, 83–100. <https://doi.org/10.1007/s10236-018-1233-x>

838 Grasso, F., Verney, R., Le Hir, P., Thouvenin, B., Schulz, E., Kervella, Y., Khojasteh Pour Fard, I.,  
839 Lemoine, J.-P., Dumas, F., Garnier, V., 2018. Suspended Sediment Dynamics in the Macrotidal  
840 Seine Estuary (France): 1. Numerical Modeling of Turbidity Maximum Dynamics. *J. Geophys.*  
841 *Res. Oceans* 123, 558–577. <https://doi.org/10.1002/2017JC013185>

842 Guisan, A., Thuiller, W., 2005. Predicting species distribution: offering more than simple habitat models.  
843 *Ecol. Lett.* 8, 993–1009. <https://doi.org/10.1111/j.1461-0248.2005.00792.x>

844 Guisan, A., Zimmermann, N.E., 2000. Predictive habitat distribution models in ecology. *Ecol. Model.*  
845 135, 147–186. [https://doi.org/10.1016/S0304-3800\(00\)00354-9](https://doi.org/10.1016/S0304-3800(00)00354-9)



846 Hale, R., Calosi, P., McNeill, L., Mieszkowska, N., Widdicombe, S., 2011. Predicted levels of future  
847 ocean acidification and temperature rise could alter community structure and biodiversity in  
848 marine benthic communities. *Oikos* 120, 661–674. [https://doi.org/10.1111/j.1600-](https://doi.org/10.1111/j.1600-0706.2010.19469.x)  
849 [0706.2010.19469.x](https://doi.org/10.1111/j.1600-0706.2010.19469.x)

850 Hayward, P.J., Ryland, J.S., 1995. *Handbook of the marine fauna of north-west Europe*. Oxford  
851 University Press.

852 He, K.S., Bradley, B.A., Cord, A.F., Rocchini, D., Tuanmu, M.-N., Schmidlein, S., Turner, W., Wegmann,  
853 M., Pettorelli, N., 2015. Will remote sensing shape the next generation of species distribution  
854 models? *Remote Sens. Ecol. Conserv.* 1, 4–18. <https://doi.org/10.1002/rse2.7>

855 Healy, T., Wang, Y., Healy, J.-A., 2002. *Muddy Coasts of the World: Processes, Deposits and Function*.  
856 Elsevier.

857 Herman, P.M.J., Middelburg, J.J., Heip, C.H.R., 2001. Benthic community structure and sediment  
858 processes on an intertidal flat: results from the ECOFLAT project. *Cont. Shelf Res., European*  
859 *Land-Ocean Interaction* 21, 2055–2071. [https://doi.org/10.1016/S0278-4343\(01\)00042-5](https://doi.org/10.1016/S0278-4343(01)00042-5)

860 Herman, P.M.J., Middelburg, J.J., Van De Koppel, J., Heip, C.H.R., 1999. Ecology of Estuarine  
861 Macrofauna, in: Nedwell, D.B., Raffaelli, D.G. (Eds.), *Advances in Ecological Research,*  
862 *Estuaries*. Academic Press, pp. 195–240. [https://doi.org/10.1016/S0065-2504\(08\)60194-4](https://doi.org/10.1016/S0065-2504(08)60194-4)

863 Huisman, J., Olff, H., Fresco, L. f. m., 1993. A hierarchical set of models for species response analysis.  
864 *J. Veg. Sci.* 4, 37–46. <https://doi.org/10.2307/3235732>

865 Hutchinson, G.E., 1957. Concluding Remarks. *Cold Spring Harb. Symp. Quant. Biol.* 22, 415–427.  
866 <https://doi.org/doi.org/10.1101/SQB.1957.022.01.039>

867 Kearney, M., Porter, W., 2009. Mechanistic niche modelling: combining physiological and spatial data  
868 to predict species' ranges. *Ecol. Lett.* 12, 334–350. [https://doi.org/10.1111/j.1461-](https://doi.org/10.1111/j.1461-0248.2008.01277.x)  
869 [0248.2008.01277.x](https://doi.org/10.1111/j.1461-0248.2008.01277.x)

870 Koenker, R., 2019. Quantile regression in r: a vignette.

871 Koenker, R., 2006. Pseudo R for Quant Reg.

872 Koenker, R., Bassett, G., 1978. Regression Quantiles. *Econometrica* 46, 33.  
873 <https://doi.org/10.2307/1913643>

874 Koenker, R., code), S.P. (Contributions to C.Q., code), P.T.N. (Contributions to S.Q., code), A.Z.  
875 (Contributions to dynrq code essentially identical to his dynlm, code), P.G. (Contributions to nlrq,  
876 routines), C.M. (author of several lnpack, advice), B.D.R. (Initial (2001) R. port from S. (to my  
877 everlasting shame--how could I. have been so slow to adopt R. and for numerous other  
878 suggestions and useful, 2019. quantreg: Quantile Regression.

879 Koenker, R., Hallock, K., 2000. Quantile regression an introduction. *J. Econ. Perspect.* 15.

880 Koenker, R., Hallock, K.F., 2001. Quantile Regression 14.

- 881 Koenker, R., Machado, J.A.F., 1999. Goodness of Fit and Related Inference Processes for Quantile  
882 Regression. *J. Am. Stat. Assoc.* 94, 1296–1310.  
883 <https://doi.org/10.1080/01621459.1999.10473882>
- 884 Łapucki, T., Normant, M., 2008. Physiological responses to salinity changes of the isopod *Idotea*  
885 *chelipes* from the Baltic brackish waters. *Comp. Biochem. Physiol. A. Mol. Integr. Physiol.* 149,  
886 299–305. <https://doi.org/10.1016/j.cbpa.2008.01.009>
- 887 Le Guen, C., Tecchio, S., Dauvin, J.-C., De Roton, G., Lobry, J., Lepage, M., Morin, J., Lassalle, G.,  
888 Raoux, A., Niquil, N., 2019. Assessing the ecological status of an estuarine ecosystem: linking  
889 biodiversity and food-web indicators. *Estuar. Coast. Shelf Sci.* 228, 106339.  
890 <https://doi.org/10.1016/j.ecss.2019.106339>
- 891 Le Hir, M., Hily, C., 2005. Macrofaunal diversity and habitat structure in intertidal boulder fields.  
892 *Biodivers. Conserv.* 14, 233–250. <https://doi.org/10.1007/s10531-005-5046-0>
- 893 Le Hir, P., Cayocca, F., Waeles, B., 2011. Dynamics of sand and mud mixtures: A multiprocess-based  
894 modelling strategy. *Cont. Shelf Res., Proceedings of the 9th International Conference on*  
895 *Nearshore and Estuarine Cohesive Sediment Transport Processes* 31, S135–S149.  
896 <https://doi.org/10.1016/j.csr.2010.12.009>
- 897 L'Ebrellec, E., Dauvin, J.-C., Bacq, N., 2019. Macrobenthos en estuaire et baie de Seine : mise à jour  
898 de la base de données MABES. Rapport d'étude réalisé par le GIP Seine-Aval. GIP Seine Aval.
- 899 Lemasson, A.J., Fletcher, S., Hall-Spencer, J.M., Knights, A.M., 2017. Linking the biological impacts of  
900 ocean acidification on oysters to changes in ecosystem services: A review. *J. Exp. Mar. Biol.*  
901 *Ecol.* 492, 49–62. <https://doi.org/10.1016/j.jembe.2017.01.019>
- 902 Lesourd, S., Lesueur, P., Fisson, C., Dauvin, J.-C., 2016. Sediment evolution in the mouth of the Seine  
903 estuary (France): A long-term monitoring during the last 150years. *Comptes Rendus Geosci.*  
904 348, 442–450. <https://doi.org/10.1016/j.crte.2015.08.001>
- 905 Lheureux, A., David, V., Del Amo, Y., Soudant, D., Auby, I., Ganthy, F., Blanchet, H., Cordier, M.-A.,  
906 Costes, L., Ferreira, S., Mornet, L., Nowaczyk, A., Parra, M., D'Amico, F., Gouriou, L.,  
907 Meteigner, C., Oger-Jeanneret, H., Rigouin, L., Rumebe, M., Tournaire, M.-P., Trut, F., Trut, G.,  
908 Savoye, N., 2022. Bi-decadal changes in nutrient concentrations and ratios in marine coastal  
909 ecosystems: The case of the Arcachon bay, France. *Prog. Oceanogr.* 201, 102740.  
910 <https://doi.org/10.1016/j.pocean.2022.102740>
- 911 Li, B., Cozzoli, F., Soissons, L.M., Bouma, T.J., Chen, L., 2017. Effects of bioturbation on the erodibility  
912 of cohesive versus non-cohesive sediments along a current-velocity gradient: A case study on  
913 cockles. *J. Exp. Mar. Biol. Ecol.* 496, 84–90. <https://doi.org/10.1016/j.jembe.2017.08.002>
- 914 Madeira, D., Fernandes, J.F., Jerónimo, D., Martins, P., Ricardo, F., Santos, A., Domingues, M.R., Diniz,  
915 M.S., Calado, R., 2021. Salinity shapes the stress responses and energy reserves of marine  
916 polychaetes exposed to warming: From molecular to functional phenotypes. *Sci. Total Environ.*  
917 795, 148634. <https://doi.org/10.1016/j.scitotenv.2021.148634>

918 Mahony, K.E., Egerton, S., Lynch, S.A., Blanchet, H., Goedknecht, M.A., Groves, E., Savoye, N., de  
919 Montaudouin, X., Malham, S.K., Culloity, S.C., 2022. Drivers of growth in a keystone fished  
920 species along the European Atlantic coast: The common cockle *Cerastoderma edule*. *J. Sea  
921 Res.* 179, 102148. <https://doi.org/10.1016/j.seares.2021.102148>

922 Malham, S.K., Hutchinson, T.H., Longshaw, M., 2012. A review of the biology of European cockles (  
923 *Cerastoderma* spp.). *J. Mar. Biol. Assoc. U. K.* 92, 1563–1577.  
924 <https://doi.org/10.1017/S0025315412000355>

925 Medeiros, I.P.M., Faria, S.C., Souza, M.M., 2020. Osmoionic homeostasis in bivalve mollusks from  
926 different osmotic niches: Physiological patterns and evolutionary perspectives. *Comp. Biochem.  
927 Physiol. A. Mol. Integr. Physiol.* 240, 110582. <https://doi.org/10.1016/j.cbpa.2019.110582>

928 Melo-Merino, S.M., Reyes-Bonilla, H., Lira-Noriega, A., 2020. Ecological niche models and species  
929 distribution models in marine environments: A literature review and spatial analysis of evidence.  
930 *Ecol. Model.* 415, 108837. <https://doi.org/10.1016/j.ecolmodel.2019.108837>

931 Mengual, B., Le Hir, P., Rivier, A., Caillaud, M., Grasso, F., 2020. Numerical modeling of bedload and  
932 suspended load contributions to morphological evolution of the Seine Estuary (France). *Int. J.  
933 Sediment Res.* 36, 723–735. <https://doi.org/10.1016/j.ijsrc.2020.07.003>

934 Morelle, J., Claquin, P., Orvain, F., 2020. Evidence for better microphytobenthos dynamics in mixed  
935 sand/mud zones than in pure sand or mud intertidal flats (Seine estuary, Normandy, France).  
936 *PLOS ONE* 15, e0237211. <https://doi.org/10.1371/journal.pone.0237211>

937 Ong, E.Z., Briffa, M., Moens, T., Van Colen, C., 2017. Physiological responses to ocean acidification  
938 and warming synergistically reduce condition of the common cockle *Cerastoderma edule*. *Mar.  
939 Environ. Res.* 130, 38–47. <https://doi.org/10.1016/j.marenvres.2017.07.001>

940 Peteiro, L.G., Woodin, S.A., Wethey, D.S., Costas-Costas, D., Martínez-Casal, A., Olabarria, C.,  
941 Vázquez, E., 2018. Responses to salinity stress in bivalves: Evidence of ontogenetic changes  
942 in energetic physiology on *Cerastoderma edule*. *Sci. Rep.* 8, 8329.  
943 <https://doi.org/10.1038/s41598-018-26706-9>

944 Richards, D., Lavorel, S., 2023. Niche theory improves understanding of associations between  
945 ecosystem services. *One Earth* 6, 811–823. <https://doi.org/10.1016/j.oneear.2023.05.025>

946 Robinson, L.M., Elith, J., Hobday, A.J., Pearson, R.G., Kendall, B.E., Possingham, H.P., Richardson,  
947 A.J., 2011. Pushing the limits in marine species distribution modelling: lessons from the land  
948 present challenges and opportunities. *Glob. Ecol. Biogeogr.* 20, 789–802.  
949 <https://doi.org/10.1111/j.1466-8238.2010.00636.x>

950 Robinson, N.M., Nelson, W.A., Costello, M.J., Sutherland, J.E., Lundquist, C.J., 2017. A Systematic  
951 Review of Marine-Based Species Distribution Models (SDMs) with Recommendations for Best  
952 Practice. *Front. Mar. Sci.* 4. <https://doi.org/10.3389/fmars.2017.00421>

- 953 Roland, A., Arduin, F., 2014. On the developments of spectral wave models: numerics and  
954 parameterizations for the coastal ocean. *Ocean Dyn.* 64, 833–846.  
955 <https://doi.org/10.1007/s10236-014-0711-z>
- 956 Saint-Béat, B., Dupuy, C., Bocher, P., Chalumeau, J., De Crignis, M., Fontaine, C., Guizien, K., Lavaud,  
957 J., Lefebvre, S., Montanié, H., Mouget, J.-L., Orvain, F., Pascal, P.-Y., Quaintenne, G.,  
958 Radenac, G., Richard, P., Robin, F., Vézina, A.F., Niquil, N., 2013. Key Features of Intertidal  
959 Food Webs That Support Migratory Shorebirds. *PLoS ONE* 8, e76739.  
960 <https://doi.org/10.1371/journal.pone.0076739>
- 961 Sauriau, P.-G., Kang, C.-K., 2000. Stable isotope evidence of benthic microalgae-based growth and  
962 secondary production in the suspension feeder *Cerastoderma edule* (Mollusca, Bivalvia) in the  
963 Marennes-Oléron Bay, in: Jones, M.B., Azevedo, J.M.N., Neto, A.I., Costa, A.C., Martins, A.M.F.  
964 (Eds.), *Island, Ocean and Deep-Sea Biology, Developments in Hydrobiology*. Springer  
965 Netherlands, Dordrecht, pp. 317–329. [https://doi.org/10.1007/978-94-017-1982-7\\_29](https://doi.org/10.1007/978-94-017-1982-7_29)
- 966 Schickele, A., Leroy, B., Beaugrand, G., Goberville, E., Hattab, T., Francour, P., Raybaud, V., 2020.  
967 Modelling European small pelagic fish distribution: Methodological insights. *Ecol. Model.* 416,  
968 108902. <https://doi.org/10.1016/j.ecolmodel.2019.108902>
- 969 Schröder, H.K., Andersen, H.E., Kiehl, K., 2005. Rejecting the mean: Estimating the response of fen  
970 plant species to environmental factors by non-linear quantile regression. *J. Veg. Sci.* 16, 373–  
971 382. <https://doi.org/10.1111/j.1654-1103.2005.tb02376.x>
- 972 Schulz, E., Grasso, F., Le Hir, P., Verney, R., Thouvenin, B., 2018. Suspended Sediment Dynamics in  
973 the Macrotidal Seine Estuary (France): 2. Numerical Modeling of Sediment Fluxes and Budgets  
974 Under Typical Hydrological and Meteorological Conditions. *J. Geophys. Res. Oceans* 123, 578–  
975 600. <https://doi.org/10.1002/2016JC012638>
- 976 Tecchio, S., Chaalali, A., Raoux, A., Tous Rius, A., Lequesne, J., Girardin, V., Lassalle, G., Cachera,  
977 M., Riou, P., Lobry, J., Dauvin, J.-C., Niquil, N., 2016. Evaluating ecosystem-level  
978 anthropogenic impacts in a stressed transitional environment: The case of the Seine estuary.  
979 *Ecol. Indic.* 61, 833–845. <https://doi.org/10.1016/j.ecolind.2015.10.036>
- 980 Thrush, S., Hewitt, J., Herman, P., Ysebaert, T., 2005. Multi-scale analysis of species-environment  
981 relationships. *Mar. Ecol.-Prog. Ser.* 302, 13–26. <https://doi.org/10.3354/Meps302013>
- 982 Thrush, S., Hewitt, J., Norkko, A., Nicholls, P., Funnell, G., Ellis, J., 2003. Habitat change in estuaries:  
983 predicting broad-scale responses of intertidal macrofauna to sediment mud content. *Mar. Ecol.*  
984 *Prog. Ser.* 263, 101–112. <https://doi.org/10.3354/meps263101>
- 985 Tillin, H.M., Tyler-Walters, H., 2016. *Cerastoderma edule* and polychaetes in littoral muddy sand: Marine  
986 Evidence-based Sensitivity Assessment (MarESA) Review. *Plymouth Mar. Biol. Assoc. U. K.*  
987 Tyler-Walters H. and Hiscock K. *Marine Life Information Network: Biology and Sensitivity Key*  
988 *Information Reviews*, [on-line]. <https://doi.org/10.17031/MARLINHAB.206.1>

- 989 Tyler-Walters, H., 2007. Common cockle (*Cerastoderma edule*): Marine Evidence-based Sensitivity  
990 Assessment (MarESA) Review. <https://doi.org/10.17031/MARLINSF.1384.1>
- 991 Ubertini, M., Lefebvre, S., Gangnery, A., Grangeré, K., Le Gendre, R., Orvain, F., 2012. Spatial  
992 Variability of Benthic-Pelagic Coupling in an Estuary Ecosystem: Consequences for  
993 Microphytobenthos Resuspension Phenomenon. *PLoS ONE* 7, e44155.  
994 <https://doi.org/10.1371/journal.pone.0044155>
- 995 Underwood, A.J., Chapman, M.G., 1996. Scales of spatial patterns of distribution of intertidal  
996 invertebrates. *Oecologia* 107, 212–224. <https://doi.org/10.1007/BF00327905>
- 997 Van Colen, C., Montserrat, F., Vincx, M., Herman, P.M.J., Ysebaert, T., Degraer, S., 2010.  
998 Macrobenthos recruitment success in a tidal flat: Feeding trait dependent effects of disturbance  
999 history. *J. Exp. Mar. Biol. Ecol.* 385, 79–84. <https://doi.org/10.1016/j.jembe.2010.01.009>
- 1000 Van Der Wal, D., Herman, P., Forster, R., Ysebaert, T., Rossi, F., Knaeps, E., Plancke, Y., Ides, S.,  
1001 2008. Distribution and dynamics of intertidal macrobenthos predicted from remote sensing:  
1002 response to microphytobenthos and environment. *Mar. Ecol. Prog. Ser.* 367, 57–72.  
1003 <https://doi.org/10.3354/meps07535>
- 1004 Weerman, E., Herman, P., van de Koppel, J., 2011. Macrobenthos abundance and distribution on a  
1005 spatially patterned intertidal flat. *Mar. Ecol. Prog. Ser.* 440, 95–103.  
1006 <https://doi.org/10.3354/meps09332>
- 1007 Weerman, E.J., van de Koppel, J., Eppinga, M.B., Montserrat, F., Liu, Q., Herman, P.M.J., 2010. Spatial  
1008 Self-Organization on Intertidal Mudflats through Biophysical Stress Divergence. *Am. Nat.* 176,  
1009 E15–E32. <https://doi.org/10.1086/652991>
- 1010 Ysebaert, T., Herman, P.M.J., 2002. Spatial and temporal variation in benthic macrofauna and  
1011 relationships with environmental variables in an estuarine, intertidal soft-sediment environment.  
1012 *Mar. Ecol. Prog. Ser.* 244, 105–124. <https://doi.org/10.3354/meps244105>
- 1013 Ysebaert, T., Meire, P., Herman, P.M.J., Verbeek, H., 2002. Macrobenthic species response surfaces  
1014 along estuarine gradients: prediction by logistic regression. *Mar. Ecol. Prog. Ser.* 225, 79–95.  
1015 <https://doi.org/10.3354/meps225079>
- 1016
- 1017

## 1018 Reference list

1019 Figure 1 Maps showing the habitats defined in the dataset of the study area. Dots represent the  
1020 location of the biological samples.

1021 Figure 2: PCA variable correlation plot with the abiotic factors' contributions in bar plots for each axis.  
1022 The red dotted line represents the mean contribution for all factors.

1023 Figure 3:  $\Delta AICc$  comparison for all SDMs computed, according to the quantile, the type of model and  
1024 the response.

1025 Figure 4: Example of modelled vs observed data plotted for each model based on biomass versus  
1026 Daily maximum current speed [ $m.s^{-1}$ ] and inundation time [%]. The black line represents the 1:1 ratio,  
1027 quantiles 0,5 in red, 0.9 in orange, 0.95 in green and 0.975 in blue.

1028 Figure 5: Examples of SDM surface plots under set A: linear with interaction (A), Gaussian non-linear  
1029 (B) and Cubic B-Spline linear (C). The upper panels show for each of the four quantiles: the biological  
1030 data observed represented by a contour plot, the model response in colour gradient surface and the  
1031 observed data over the model are represented by red stars; the lower panel shows the 3D plots with all  
1032 processed quantiles superposed.

1033 Figure 6: Sets of quantile regression models with 2 crossed abiotic factors (A,B,C and D see 3.2)  
1034 computed with linear model (top row, numbered 1) and non-linear with the Gaussian equation (bottom  
1035 row, numbered 2), the observed biological data under the model surface are represented by an isometric  
1036 curve, the data over the model are represented by red stars. Each pair has its own range of biomass to  
1037 ensure visibility.

1038 Figure 7: SDM models suitability index applied on the Seine estuary over the five periods.

1039 Figure 8: Abiotic factors and resulting SDM suitability index per period and per area for all SDM  
1040 models with a 95% confidence interval.

1041

## 1042 Table list

1043 Table 1 List of types of models tested

1044 Table 2 PCA scores for abiotic factors

1045